TRENDS IN SCIENCES 2026; 23(12): 14577
https://doi.org/10.48048/tis.2026.14577 RESEARCH ARTICLE

Pangasius micronemus Oil: Extraction Method Comparison, Fatty Acid Profile, and Biological Evaluation in A549 and Huh-7 Cancer

Anggita Rosiana Putri[1,2,*], Nathaniel Indra Hentyan[1], Risma Ainun Nisa[1], Salma Izzah Abidah[1], Luthfi Ahmad Muchlashi[1,2], Prisma Trida Hardani[1,2], Kevin Awidarta[1] and Leena Suntornsuk[3]

[1]*Department of Pharmacy, Faculty of Medicine, Universitas Brawijaya, Malang 65145, Indonesia*
[2]*Drug Development and Analytical Methods Research Group, Faculty of Medicine, Universitas Brawijaya, Malang 65145, Indonesia*
[3]*Department of Pharmaceutical Chemistry, Faculty of Pharmacy, Mahidol University, Bangkok 10400, Thailand*

([*]Corresponding author's e-mail: anggita.rosiana@ub.ac.id)

Received: 3 June 2026, Revised: 16 June 2026, Accepted: 26 June 2026, Published: 5 August 2026

Abstract

Pangasius micronemus oil (PMO) has attracted attention as a potential source of bioactive lipids with nutraceutical value; however, its quality and biological activity are highly dependent on the extraction method. This study aimed to characterize the physicochemical properties and fatty acid composition of PMO obtained by mechanical pressing and Soxhlet extraction, and to evaluate its anticancer potential through integrated *in vitro* and *in silico* approaches. Physicochemical properties were evaluated according to Association of Official Analytical Chemists (AOAC) official methods and fatty acid profiles were determined by gas chromatography with flame ionization detection (GC–FID). Cytotoxic activity was evaluated via 3-(4,5-dimethylthiazol-2-yl)-2,5-diphenyltetrazolium bromide (MTT) assay on A549 (non-small cell lung cancer, NSCLC) and Huh-7 (hepatocellular carcinoma) cell lines. Molecular docking and network pharmacology analyses were subsequently performed to explore potential mechanisms of action against NSCLC-related targets. Soxhlet extraction yielded higher oil content (29.57%) than mechanical pressing (25.79%) ($p < 0.05$); however, pressed oil demonstrated good physicochemical quality, with lower acid value (6.07 mg KOH/g), lower peroxide value (2.33 meq O_2/kg), higher saponification value (188 mg KOH/g), and higher iodine value (74.22 g I_2/100 g). Fatty acid profiles were highly similar between extraction methods, with unsaturated fatty acids accounting for 63.60% - 64.64% of total fatty acids. Oleic acid was the predominant fatty acid (43.57% - 44.11%), followed by palmitic acid (29.14% - 29.22%) and linoleic acid (15.21% - 15.55%). Biological evaluation demonstrated weak cytotoxic activity against A549 cells, with an estimated IC_{50} value of 4,520 ± 3,190 µg/mL, and no significant inhibitory effect against Huh-7 cells across the tested concentration range. Molecular docking revealed that docosahexaenoic acid (DHA) displayed the strongest binding affinities toward epidermal growth factor receptor (EGFR), mammalian target of rapamycin (mTOR), and matrix metalloproteinase-9 (MMP-9), while network pharmacology identified multiple cancer-related targets and pathways associated with lipid metabolism and cell proliferation. These findings indicate that mechanical pressing yielded oil with favorable physicochemical characteristics, while PMO demonstrated limited direct anticancer activity under the conditions tested.

Keywords: *Pangasius micronemus*, Fish oil, Mechanical pressing, Soxhlet extraction, Fatty acid composition, Physicochemical properties, A549 cells, Huh-7 cells

Introduction

Fish oil has been widely recognized as a valuable source of bioactive lipids, particularly polyunsaturated fatty acids (PUFAs), which have been associated with various health-promoting properties including anti-inflammatory, cardioprotective, and potential anticancer effects [1-4]. Among freshwater fish species native to Southeast Asia, especially in Indonesia, *Pangasius micronemus* represents an economically significant resource whose lipid fraction remains underexplored relative to its nutritional and biomedical potential. Preliminary investigations have indicated that PMO contains unsaturated fatty acids, including linoleic acid, oleic acid, and trace amounts of long-chain omega-3 fatty acids such as eicosapentaenoic acid (EPA) and docosahexaenoic acid (DHA) [5-7]. These fatty acids have been reported to participate in the regulation of cellular pathways relevant to cancer biology, including apoptosis induction, cell cycle modulation, and inhibition of pro-inflammatory signaling [8].

Lung cancer remains one of the of the leading causes of cancer-related mortality worldwide. The GLOBOCAN 2020 report estimated approximately 2.2 million new cases and 1.8 million deaths annually, with NSCLC accounting for the majority of cases [9]. Current therapeutic strategies, including targeted therapy and immunotherapy, have improved survival outcomes; however, challenges such as acquired drug resistance, systemic toxicity, and tumor heterogeneity continue to limit long-term efficacy [10,11]. These limitations have have stimulated interest in naturally derived compounds that may serve as complementary agents capable of modulating multiple molecular targets simultaneously. In parallel, HCC represents a significant global health burden, ranking among the leading causes of cancer-related mortality with limited treatment options in advanced stages [12,13]. Emerging evidence suggests that dietary lipids, particularly omega-3 and omega-6 fatty acids, may modulate hepatic cancer cells behaviour. These effects are thought to involve lipid metabolism reprogramming, oxidative stress regulation, and activation of apoptotic pathways [14]. Given its fatty acid profile, PMO warrants systematic evaluation against both NSCLC and HCC cell lines, though its direct cytotoxic potential remains to be established.

The biological activity of fish oil is closely linked to its fatty acid composition, particularly the relative abundance of omega-3 and omega-6 fatty acids [15]. Long-chain omega-3 fatty acids, notably EPA and DHA, have been reported to suppress tumor cell proliferation through induction of apoptosis, cell cycle arrest, and downregulation of oncogenic signaling pathways such as PI3K/Akt and NF-κB [8]. In contrast, an excess of omega-6 fatty acids may promote a pro-inflammatory microenvironment conducive to tumor progression via eicosanoid-mediated mechanisms [16]. Consequently, differences in fatty acid composition arising from the extraction method employed may have direct implications for the biological activity of the resulting oil.

The extraction method is a critical determinant of both the yield and quality of fish oil. Soxhlet extraction is among the most widely used conventional techniques due to its high extraction efficiency; however, prolonged thermal exposure and organic solvent contact may accelerate lipid oxidation, elevate free fatty acid content, and compromise the integrity of thermolabile bioactive constituents [17]. Mechanical pressing, by contrast, offers a solvent-free alternative that minimizes thermal stress and aligns with sustainable processing principles, though it generally yields lower oil recovery [18]. Despite the recognized importance of extraction conditions, studies that systematically link extraction method to physicochemical quality and downstream biological activity remain limited, representing a critical gap in the current literature.

To complement experimental findings, computational approaches have increasingly been integrated into natural product research. Molecular docking enables the prediction of binding interactions between bioactive ligands and target proteins at the atomic level, while network pharmacology provides a systems-level perspective on multi-target mechanisms of action [19]. In the context of NSCLC, proteins such as EGFR, mTOR, and MMP-9 are well-established regulators of tumor proliferation, survival, and invasion [20]. Despite the growing body of literature on fish oil bioactivity, studies that systematically examine the molecular interactions of fish oil–derived fatty acids with these targets and subsequently contextualize them within NSCLC-relevant biological networks remain

scarce, underscoring the rationale for the integrated *in silico* approach adopted in the present study.

To the best of our knowledge, this is the first study that comprehensively integrates extraction method comparison, physicochemical characterization, fatty acid profiling, *in vitro* cytotoxicity evaluation, molecular docking, and network pharmacology analysis of PMO within a unified analytical framework. This study therefore aimed to: (i) compare mechanical pressing and Soxhlet extraction with respect to oil yield and physicochemical quality; (ii) determine fatty acid composition by GC–FID; (iii) evaluate *in vitro* cytotoxic activity against A549 (NSCLC) and Huh-7 (HCC) cell lines using the MTT assay; (iv) investigate molecular interactions of major PMO fatty acids with NSCLC-related target proteins via molecular docking; and (v) elucidate the molecular interactions and multi-target mechanisms of PMO fatty acids against NSCLC-related targets through integrated molecular docking and network pharmacology analyses.

Materials and methods

Materials and chemicals

Pangasius micronemus samples were obtained from Ngunut Village (8.105° S, 111.902° E) in August 2025. The fish were collected and processed within 24 - 48 h post-harvest to preserve sample integrity. Prior to analysis, the fish were manually dissected, and only the muscle tissue (fillet) was retained, while non-edible parts, including the head, fins, viscera, and bones, were removed. The prepared samples were then stored at −20 °C until further analysis.

All chemicals and reagents were of analytical grade. Potassium hydroxide (KOH), hydrochloric acid (HCl), sodium thiosulfate ($Na_2S_2O_3$), potassium iodide (KI), Wijs reagent, acetic acid, chloroform, n-hexane, diethyl ether, petroleum ether, heptane, sodium methoxide, boron trifluoride methanolate, phenolphthalein, and starch indicator were purchased from Sigma-Aldrich (St. Louis, MO, USA). For cell-based assays, Ham's F-12 Nutrient Mix, Dulbecco's Modified Eagle Medium (DMEM), trypsin–EDTA solution, and MTT reagent were obtained from Sigma-Aldrich. Fetal bovine serum (FBS) was purchased from Biowest (Nuaillé, France), and penicillin–streptomycin solution was obtained from Sigma-Aldrich. Dimethyl sulfoxide (DMSO) used as vehicle solvent was also sourced from Sigma-Aldrich. Fatty acid methyl ester (FAME) standards for GC–FID identification were obtained from Supelco (Bellefonte, PA, USA). For molecular docking, structures of major fatty acids including EPA, DHA, α-linolenic acid (ALA), γ-linolenic acid (GLA), linoleic acid (LA), and oleic acid (OA) were retrieved from the PubChem database (https://pubchem.ncbi.nlm.nih.gov/).

Oil extraction

Soxhlet extraction

Prior to extraction, fillets were dried at 60 °C until constant weight was achieved, then ground into a fine powder using a mechanical grinder. A total of 100 g of the dried powdered material was placed in a cellulose thimble and subjected to Soxhlet extraction using 250 mL of n-hexane as the solvent for 6 hours at the solvent's reflux temperature. Following extraction, the solvent was removed using a rotary evaporator (40 °C, 80 rpm) until no residual solvent was detectable by odor. The resulting oil was collected and stored at −20 °C until further analysis.

Mechanical pressing

Mechanical extraction was performed using a screw press machine. The fresh fish fillets were fed directly into the press at an operating temperature not exceeding 50 °C, a screw rotation speed of 30 rpm, and an applied pressure of approximately 150 bar. The generated pressure and frictional force within the helical chamber released the oil, which was subsequently collected and filtered through a 0.45 µm membrane filter to remove solid residues. The resulting oil was stored at −20 °C until further analysis.

Extraction yield

The oil yield from each extraction method was determined gravimetrically. The extraction yield was calculated as follows:

$$\text{Yield (\%)} = \frac{\text{mass of extracted oil (g)}}{\text{mass of initial raw material (g)}} \times 100\% \quad (1)$$

All extractions were performed in triplicate, and results were expressed as mean ± standard deviation (SD).

Physicochemical property characterization

All physicochemical analyses were conducted in accordance with the official methods of AOAC and performed in triplicate unless otherwise stated. Results are expressed as mean ± SD.

Acid value

The acid value (AV) was determined by direct titration according to AOAC Official Method 940.28 [21]. A 5 g oil sample was dissolved in 50 mL of neutralized 95% ethanol and titrated against 0.1 N KOH using phenolphthalein as an indicator. The endpoint was defined as the appearance of a persistent pale pink coloration. The AV was expressed as mg KOH per gram of oil (mg KOH/g).

Peroxide value

The peroxide value (PV) was determined by iodometric back-titration according to AOAC Official Method 965.33 [22]. A 5 g oil sample was dissolved in 30 mL of acetic acid–chloroform (3:2, v/v) and treated with saturated KI solution under exclusion of light. Following the addition of distilled water, liberated iodine was titrated against 0.01 N $Na_2S_2O_3$ using starch solution as an indicator to a colorless endpoint. The PV was expressed as milliequivalents of active oxygen per kilogram of oil (meq O_2/kg).

Saponification value

The saponification value (SV) was determined by reflux saponification followed by back-titration according to AOAC Official Method 920.160 [22]. A 2 g oil sample was refluxed with 25 mL of 0.5 N alcoholic KOH for 60 min to ensure complete saponification. Upon cooling to room temperature, the excess KOH was back-titrated with 0.5 N hydrochloric acid (HCl) in the presence of phenolphthalein until the pink color dissipated. A reagent blank was processed simultaneously under identical conditions. The SV was expressed as milligrams of KOH per gram of oil (mg KOH/g).

Iodine value

The iodine value (IV) was determined using the Wijs method according to AOAC Official Method 993.20 [22]. A 0.5 g oil sample was dissolved in chloroform and treated with an excess of Wijs reagent, followed by incubation in the dark for 30 min to allow complete halogenation. Potassium iodide (KI) solution and distilled water were subsequently added, and the liberated iodine was titrated against 0.1 N $Na_2S_2O_3$ using starch solution as an indicator to a colorless endpoint. A reagent blank was carried through the procedure under identical conditions. The IV was expressed as grams of iodine absorbed per 100 g of oil (g I_2/100 g).

Fatty acid composition analysis by GC-FID

Prior to GC–FID analysis, the PMO was hydrolyzed and methylated to obtain fatty acid methyl esters (FAMEs) following the previous method [7]. Briefly, 5 g of oil was hydrolyzed with 10 mL of concentrated HCl at 80 °C for 3 h, cooled to room temperature, and extracted using a mixture of diethyl ether and petroleum ether (1:1, v/v). The organic phase was evaporated under a stream of nitrogen, and 0.5 mL of the resulting residue was methylated with sodium methoxide and boron trifluoride methanolate at 60 °C for 30 min. FAMEs were subsequently extracted with heptane and saturated NaCl solution, and the upper organic layer was transferred into GC vials for analysis.

GC–FID analysis was performed using an Agilent Technologies 7890B gas chromatograph equipped with an HP-88 capillary column (100 m×0.30 mm i.d., 0.20 μm film thickness). The injector and detector temperatures were maintained at 240 and 250 °C, respectively. Samples were injected in split mode at a ratio of 10:1. Helium was used as the carrier gas at a constant flow rate of 1.0 mL/min, with nitrogen as the makeup gas. The oven temperature program was as follows: Initial temperature of 100 °C held for 1 min, increased at a rate of 2 °C/min to 240 °C, and held for 9 minutes, resulting in a total run time of 80 min. Individual fatty acids were identified by comparing retention times with FAME reference standards, and results were expressed as relative percentage of total fatty acids.

***In vitro* cytotoxicity assessment**

Cell culture

The A549 human lung adenocarcinoma cell line was cultured in Ham's F-12 Nutrient Mix, and Huh-7 human hepatocellular carcinoma cells were maintained in DMEM. Both media were supplemented with 10% FBS and 1% penicillin–streptomycin. Cells were

maintained at 37 °C in a humidified incubator with 5% CO_2. Upon reaching approximately 80% confluence, cells were subcultured using trypsin–EDTA solution and passaged into new culture flasks to maintain exponential growth phase.

Sample preparation

A total of 10 mg of PMO was dissolved in 100 µL of DMSO to prepare a stock solution at a concentration of 100,000 µg/mL. Serial dilutions were subsequently prepared in complete culture medium to yield final working concentrations of 1000, 750, 500, 250, 100, 50, 10, 1, 0.1, and 0.01 µg/mL. The final DMSO concentration in all treatment wells was maintained at ≤ 0.1% (v/v) to preclude solvent-induced cytotoxic effects, as confirmed by a vehicle control group.

MTT cytotoxicity assay

Cytotoxicity was evaluated using the MTT assay. Cells were seeded in 96-well microplates at a density of 1×10^4 cells/well and allowed to adhere for 24 h prior to treatment. Following adherence, the culture medium was replaced with medium containing the respective PMO concentrations, and cells were incubated for 48 h at 37 °C with 5% CO_2. After the treatment period, the medium was aspirated and replaced with 150 µL of culture medium containing 15 µL of MTT solution (0.5×10^3 µg/mL). Plates were incubated for an additional 4 h to allow formazan crystal formation by metabolically active cells. The formazan crystals were dissolved by adding 100 µL of DMSO per well, followed by gentle agitation in the dark for 20 min at room temperature.

Absorbance was measured at 560 nm (test wavelength) and 750 nm (reference wavelength) using a GloMax Microplate Multidetection Reader (Promega, Madison, WI, USA). Cell viability was calculated as follows:

$$Cell\ Viability\ (\%) = \frac{A\ treatment}{A\ control} \times 100 \quad (2)$$

where A treatment and A control represent the absorbance values of treated and untreated control wells, respectively.

All assays were performed in triplicate, and results were expressed as mean ± SD. The 50% inhibitory concentration (IC_{50}) was determined using probit regression analysis in IBM SPSS Statistics (version 26.0). Concentration data were $\log_{10}$-transformed prior to analysis to linearize the dose–response relationship, and IC_{50} values were derived from the regression equation at the point corresponding to 50% inhibition (probit value = 5).

Molecular docking

Ligand and protein preparation

The 3-dimensional structures of major PMO fatty acids EPA, DHA, ALA, GLA, LA, and OA were retrieved from the PubChem database in SDF format and imported into PyRx (version 0.8) for energy minimization using the Universal Force Field (UFF) prior to docking. Target protein structures associated with NSCLC pathogenesis, specifically EGFR (PDB ID: 5D41), mTOR (PDB ID: 4DRI), and MMP-9 (PDB ID: 5UE4), were retrieved from the RCSB Protein Data Bank (https://www.rcsb.org/). Protein preparation was performed using UCSF Chimera (version 1.16), including removal of water molecules, addition of hydrogen atoms, and assignment of Gasteiger charges. Native ligands co-crystallized within each protein structure were retained for docking validation purposes.

Docking validation and execution

Docking validation was performed by redocking the native ligand of each target protein into its original binding site using AutoDock Vina (version 1.1.2). Docking protocols were considered validated when the root mean square deviation (RMSD) between the redocked and crystallographic poses was less than 2.0 Å, indicating acceptable reproduction of the experimental binding mode. Grid box dimensions and coordinates were defined based on the binding site of each co-crystallized native ligand. Molecular docking of PMO fatty acids was subsequently performed under identical grid parameters. Protein–ligand interaction profiles, including binding modes, interaction types (hydrogen bonds, hydrophobic contacts, van der Waals interactions), and involved amino acid residues, were visualized and analyzed using BIOVIA Discovery Studio Visualizer (version 21.1.0) in both 2-dimensional (2D) and 3-dimensional (3D) representations.

Network pharmacology

Potential targets of fatty acids present at levels above 1%, as determined by GC-FID analysis, were retrieved from SwissTargetPrediction (https://www.swisstargetprediction.ch/) under the conditions of Homo sapiens and probability > 0 and SuperPRED (https://prediction.charite.de/). Potential targets associated with NSCLC were obtained from the Therapeutic Target Database (https://ttd.idrblab.cn/) and Comparative Toxicogenomics Database (https://ctdbase.org/) with marker/mechanism criteria. All identified fatty acid and NSCLC targets were then analyzed using the Jvenn diagram tool (https://jvenn.toulouse.inrae.fr/app/index.html) to visualize their intersections. The overlapping targets between fatty acids and NSCLC were subsequently imported into the STRING database (https://cn.string-db.org/) for protein–protein interaction (PPI) analysis, using Homo sapiens as the selected organism and a minimum required interaction score of 0.4. The resulting PPI network was visualized and further analyzed using Cytoscape software (v3.10.1). Topological properties of the network were evaluated by calculating degree values using the CytoHubba plugin within Cytoscape. Functional enrichment analysis, including Gene Ontology (GO) and Kyoto Encyclopedia of Genes and Genomes (KEGG) pathway analysis, was performed using SRPLOT (https://www.bio informatics.com.cn/en). GO analysis was conducted to identify biological processes (BP), cellular components (CC), and molecular functions (MF). In contrast, KEGG pathway enrichment analysis was used to determine key signaling pathways involved in the biological processes.

Statistical analysis

Data from extraction yield and physicochemical characterization were analyzed using IBM SPSS Statistics (version 27.0). Normality of data distribution was assessed using the Shapiro–Wilk test, appropriate for sample sizes fewer than 50 observations. For normally distributed data ($p > 0.05$), homogeneity of variance was further evaluated using Levene's test. When variances were homogeneous ($p > 0.05$), differences between extraction methods were assessed using an independent samples *t*-test assuming equal variances; when variances were heterogeneous, Welch's *t*-test was applied. For data that did not meet the normality assumption ($p < 0.05$), the Mann–Whitney U test was employed as a non-parametric alternative. Statistical significance was defined at $p < 0.05$ for all analyses.

Results and discussion

Oil extraction yield

Extraction of *Pangasius micronemus* muscle tissue by 2 distinct methods yielded oils with notably different recovery rates. Soxhlet extraction produced a higher oil yield (29.57 ± 1.46%) than mechanical pressing (25.79 ± 1.02%), and this difference was statistically significant (independent samples *t*-test, $p = 0.021$), as summarized in **Table 1**. The higher yield obtained by Soxhlet extraction may be attributed to continuous solvent recirculation through the sample matrix, which facilitates more complete solubilization and recovery of lipids entrapped within cellular structures, including bound and structural lipids that are not readily released by mechanical force alone [23]. These findings are consistent with previous reports by Hagbe *et al.* [24], who reported that solvent-based extraction methods generally yield higher oil recovery than mechanical methods.

However, a higher yield does not necessarily reflect better oil quality. Prolonged thermal exposure and repeated solvent contact during Soxhlet extraction can promote lipid hydrolysis, accelerate oxidative reactions, and co-extract non-lipid impurities, all of which may compromise the physicochemical integrity of the resulting oil [26]. This trade-off between yield and quality is a recurring finding in fish oil extraction literature and underscores the importance of evaluating both parameters in tandem rather than optimizing yield alone. The physicochemical implications of this trade-off are examined in detail in the following section.

Table 1 Comparative physicochemical properties of PMO obtained by mechanical pressing and Soxhlet extraction.

Parameter	Unit	Mechanical Pressing (Mean ± SD, n = 3)	Soxhlet Extraction (Mean ± SD, n = 3)
Yield	%	25.79 ± 1.02[a]	29.57 ± 1.46[b]
Acid Value (AV)	mg KOH/g	6.07 ± 0.13[a]	7.38 ± 0.07[b]
Peroxide Value (PV)	meq O_2/kg	2.33 ± 0.12[a]	3.73 ± 0.12[b]
Saponification Value (SV)	mg KOH/g	188.85 ± 9.22[b]	160.89 ± 0.57[a]
Iodine Value (IV)	g I_2/100 g	74.22 ± 0.53[b]	70.70 ± 2.10[a]

Note: Values are expressed as mean ± SD (n = 3). Different superscript letters (a,b) within the same row indicate statistically significant differences between extraction methods ($p < 0.05$), whereas identical letters indicate no significant difference.

Physicochemical characteristic of PMO

Acid value

The acid value (AV) reflects the concentration of free fatty acids (FFA) in an oil and serves as a primary indicator of hydrolytic degradation. As shown in **Table 1**, Soxhlet-extracted PMO exhibited a substantially higher AV (7.38 ± 0.07 mg KOH/g) compared with oil obtained by mechanical pressing (6.07 ± 0.13 mg KOH/g), and this difference was statistically significant (Mann–Whitney U test, $p = 0.046$). The markedly elevated AV in Soxhlet-extracted oil is consistent with accelerated triglyceride hydrolysis resulting from prolonged thermal exposure and repeated solvent cycling, both of which promote ester bond cleavage and FFA liberation [25-27].

When evaluated against the quality standard established by the Codex Alimentarius Commission for crude fish oil (Codex Stan 329-2017), which specifies a maximum AV of 3.0 mg KOH/g for crude fish oil intended for further processing, both extraction methods exceeded this threshold. However, the AV of pressed oil (6.07 mg KOH/g) was considerably lower than that of Soxhlet-extracted oil (51.66 mg KOH/g), indicating relatively better preservation of lipid integrity under mechanical extraction conditions. Both oils would require a degumming and neutralization step prior to use as a nutraceutical ingredient to reduce FFA content to acceptable levels [28].

The substantially lower AV in pressed oil aligns with the green chemistry rationale underlying mechanical extraction the absence of organic solvents and the lower thermal load minimize conditions that would otherwise promote triglyceride hydrolysis [29]. These findings are consistent with Rahman *et al.*, who reported that solvent-based extraction was associated with significantly higher FFA content relative to solvent-free methods, attributing this difference to the combined effect of heat and solvent polarity on lipid ester bond stability [12, 30].

Peroxide value

The peroxide value (PV) measures the concentration of primary oxidation products (hydroperoxides) in an oil and is widely used as an early indicator of lipid oxidative deterioration. As presented in **Table 1**, Soxhlet-extracted PMO showed a higher mean PV (3.73 ± 0.12 meq O_2/kg) than pressed oil (2.33 ± 0.11 meq O_2/kg), with a statistically significant difference confirmed by the Mann–Whitney U test ($p = 0.043$). Both values fall within the acceptable range specified by the Codex Alimentarius Commission for crude fish oil (maximum PV of 5 meq O_2/kg; Codex Stan 329-2017), indicating that neither extraction method induced severe primary oxidation under the conditions employed [28].

Nevertheless, the higher PV in Soxhlet-extracted oil suggests that continuous heating during extraction promotes hydroperoxide formation through thermally induced lipid oxidation, even within the relatively short extraction window employed in this study [31]. Hydroperoxides, while not directly harmful at low concentrations, are unstable intermediates that decompose into secondary oxidation products such as aldehydes and ketones, which contribute to off-flavors and potential cytotoxicity in lipid-based nutraceuticals. From a nutraceutical quality perspective, the lower PV

observed in pressed oil indicates better preservation of oxidative stability, which is particularly relevant given the high PUFA content of PMO. PUFAs are inherently susceptible to oxidative degradation due to the presence of multiple double bonds. The pressing method, by avoiding organic solvent exposure and operating at lower thermal conditions, appears to better preserve the oxidative integrity of the oil.

Saponification value

The saponification value (SV) reflects the average molecular weight of fatty acids esterified within triglycerides — higher values indicate a greater proportion of short- to medium-chain fatty acids, while lower values are associated with predominantly long-chain fatty acids [32]. Pressed PMO exhibited a higher mean SV (188.85 ± 9.22 mg KOH/g) than Soxhlet-extracted oil (160.89 ± 0.57 mg KOH/g), a difference that was statistically significant (independent samples *t*-test, $p = 0.021$).

When compared with the reference SV range for fish oil reported by American Society for Testing and Materials (ASTM, 1952) is in the range of 175 - 201 mg KOH g^{-1} [30], pressed PMO fell within the acceptable range, whereas Soxhlet-extracted oil fell below this range. The lower SV in Soxhlet-extracted oil may reflect partial triglyceride degradation during prolonged extraction, as well as the possible co-extraction of long-chain wax esters and non-saponifiable lipids that dilute the saponifiable fraction and lower the overall SV [31]. In contrast, the mechanical pressing process, which involves neither solvent nor prolonged heating, better preserves the native triglyceride composition of the oil, as reflected by the SV within the expected range for intact fish oil. From a quality assurance perspective, SV within the reference range serves as an indirect confirmation of triglyceride purity and minimal lipid degradation, both of which are desirable characteristics for a nutraceutical-grade oil.

Iodine value

The iodine value (IV) quantifies the degree of unsaturation in an oil by measuring the amount of iodine absorbed per 100 g, with higher values indicating greater unsaturated fatty acid (UFA) content [32]. Pressed PMO exhibited a slightly higher IV (74.22 ± 0.53 g I_2/100 g) than Soxhlet-extracted oil (70.71 ± 2.10 g I_2/100 g), and this difference was statistically significant (Mann–Whitney U test, $p = 0.046$).

Both values are considerably lower than the IV range of 145 - 180 g I_2/100 g specified for refined cod liver oil under USP (US Pharmacopeia) [33]. However, direct comparison with this reference is not entirely appropriate, as *Pangasius micronemus* is a freshwater tropical species whose fatty acid composition differs fundamentally from cold-water marine species such as cod — tropical freshwater fish oils are generally characterized by a lower proportion of long-chain PUFAs (EPA and DHA) and a higher proportion of C18 unsaturated fatty acids such as linoleic and oleic acid, which naturally yield lower IV [34]. The IV values reported here are therefore more appropriately contextualized against tropical freshwater fish oil literature, where comparable IV ranges have been reported for *Pangasius* species and similar catfish [35]. The slightly higher IV in pressed oil suggests better retention of unsaturated fatty acids, consistent with the lower thermal exposure in mechanical pressing, which reduces oxidative degradation of double bonds during extraction.

Taken together, the physicochemical data indicate that while Soxhlet extraction produces higher oil yield, mechanical pressing consistently yields oil of superior quality across all 4 parameters evaluated. The lower acid value, lower peroxide value, higher saponification value, and slightly higher iodine value of pressed PMO collectively suggest better preservation of lipid integrity, reduced hydrolytic and oxidative degradation, and more favorable chemical composition for nutraceutical application. These differences are directly attributable to the fundamental differences in extraction conditions — the absence of organic solvent, lower operating temperature, and shorter effective processing time in mechanical pressing collectively minimize the degradation pathways that compromise oil quality in solvent-based methods. Nonetheless, both oils exceed crude fish oil quality thresholds for acid value and would require further refining prior to nutraceutical use.

Fatty acids profiles

The fatty acid profiles of PMO obtained by pressing and Soxhlet extraction are presented in **Table 2**. Both extraction methods yielded oils with remarkably similar fatty acid profiles, suggesting that the extraction

technique exerted minimal influence on the overall lipid composition. In both samples, unsaturated fatty acids (UFAs) constituted the predominant fraction, accounting for 63.60% and 64.64% of total fatty acids in the pressing and Soxhlet extracts, respectively, whereas saturated fatty acids (SFAs) represented 34.67% and 35.28%.

Among the SFAs, palmitic acid (C16:0) was the dominant component, contributing approximately 29% of total fatty acids in both extraction methods. This finding is consistent with previous reports on freshwater catfish species, in which palmitic acid is frequently identified as the major saturated fatty acid [38]. The predominance of palmitic acid reflects its fundamental role in fish lipid metabolism and energy storage. Myristic acid (C14:0) was the second most abundant SFA, accounting for approximately 3.6% - 3.8%, whereas the remaining saturated fatty acids were detected only in minor quantities (< 1%). Interestingly, heptadecanoic acid (C17:0) was detected exclusively in the Soxhlet extract, suggesting that solvent-assisted extraction may improve the recovery of trace lipid constituents that are less efficiently extracted through mechanical pressing.

A notable characteristic of *P. micronemus* oil is the predominance of monounsaturated fatty acids (MUFAs), particularly oleic acid (C18:1, ω-9), which represented 44.11% and 43.46% of total fatty acids in the pressing and Soxhlet extracts, respectively. The exceptionally high abundance of oleic acid indicates that *P. micronemus* oil possesses a lipid profile more closely resembling oleic-rich edible oils than conventional marine fish oils, which are generally characterized by elevated levels of long-chain ω-3 polyunsaturated fatty acids (PUFAs). Oleic acid has been extensively associated with beneficial physiological effects, including modulation of plasma lipid profiles, reduction of low-density lipoprotein oxidation, and attenuation of inflammatory responses. Consequently, the high oleic acid content may contribute substantially to the nutritional and functional value of the oil.

Linoleic acid (C18:2, ω-6) was the second most abundant unsaturated fatty acid, accounting for 15.21% and 15.55% in the pressing and Soxhlet extracts, respectively. Together with γ-linolenic acid and arachidonic acid, it forms the major ω-6 fatty acid fraction in the oil. The relatively high proportion of linoleic acid is characteristic of freshwater fish species, whose dietary sources often contain greater amounts of terrestrial plant-derived lipids than marine food webs. The presence of these essential fatty acids is nutritionally relevant because they serve as precursors for the biosynthesis of eicosanoids involved in cellular signaling, immune regulation, and inflammatory processes.

Although present at lower concentrations, the ω-3 fatty acids identified in *P. micronemus* oil deserve particular attention. α-Linolenic acid (ALA) was detected at 1.09% - 1.16%, while DHA accounted for 0.27% - 0.28% of total fatty acids. The relatively low DHA content contrasts with marine fish oils but is consistent with the fatty acid profiles typically reported for freshwater species. Nevertheless, the occurrence of DHA remains significant due to its established role in neural development, cognitive function, visual acuity, and cardiovascular health. The simultaneous presence of both ω-3 and ω-6 essential fatty acids suggests that *P. micronemus* oil may serve as a complementary dietary lipid source with potential functional food applications.

The overall UFA/SFA ratios were 1.83 for both extraction methods, indicating a predominance of unsaturated lipids regardless of the extraction technique employed. Such a ratio is generally regarded as favorable from a nutritional perspective because higher proportions of unsaturated fatty acids are associated with improved cardiovascular health outcomes. Furthermore, the calculated ω-6/ω-3 ratios were 12.30 and 12.09 for the pressing and Soxhlet extracts, respectively. Although these values exceed those typically observed in marine fish oils, they are comparable to ratios reported for other freshwater fish species. The similarity of these nutritional indices further demonstrates that mechanical pressing effectively preserves the lipid quality of the oil.

Comparison of the 2 extraction methods revealed only marginal quantitative differences in fatty acid composition. Soxhlet extraction resulted in slightly higher concentrations of total UFAs, γ-linolenic acid, α-linolenic acid, nervonic acid, and arachidonic acid. This observation is likely attributable to the enhanced solvating power of organic solvents, which facilitates the recovery of lipid fractions embedded within cellular matrices. However, the differences were relatively small and did not substantially alter the nutritional profile of

the oil. From a practical standpoint, these findings are particularly important because they demonstrate that pressing, a solvent-free and environmentally sustainable extraction technique, can produce oil with a fatty acid composition comparable to that obtained by conventional solvent extraction.

Table 2 GC–FID characterization of saturated and unsaturated fatty acids in *PMO* extracted by pressing and Soxhlet methods.

Fatty Acid	Structure	Pressing (% relative, mean ± SD)	Soxhlet Extraction (% relative, mean ± SD)
Saturated Fatty Acids (SFA)			
Lauric acid	C12:0	0.42 ± 0.00	0.31 ± 0.00
Myristic acid	C14:0	3.61 ± 0.00	3.78 ± 0.00
Pentadecanoic acid	C15:0	0.17 ± 0.01	0.18 ± 0.00
Palmitic acid	C16:0	29.14 ± 0.00	29.22 ± 0.00
Heptadecanoic acid	C17:0	0.00	0.23 ± 0.00
Arachidic acid	C20:0	0.26 ± 0.00	0.27 ± 0.00
Heneicosanoic acid	C21:0	0.10 ± 0.00	0.24 ± 0.00
Docosanoic acid	C22:0	0.11 ± 0.00	0.11 ± 0.00
Tricosanoic acid	C23:0	0.77 ± 0.00	0.84 ± 0.00
Lignoceric acid	C24:0	0.09 ± 0.00	0.10 ± 0.00
Total SFA		**34.67**	**35.28**
Unsaturated Fatty Acids (UFA)			
Palmitoleic acid	C16:1	1.09 ± 0.00	1.04 ± 0.00
Oleic acid	C18:1 (ω-9)	44.11 ± 0.00	43.57 ± 0.06
Linoleic acid	C18:2 ((ω-6)	15.21 ± 0.00	15.55 ± 0.00
γ-Linolenic acid	C18:3 (ω-6)	1.52 ± 0.00	1.75 ± 0.00
Cis-11-Eicosenoic acid	C20:1 (ω-9)	0.65 ± 0.00	0.61 ± 0.00
α-Linolenic acid	C18:3 (ω-3)	1.09 ± 0.00	1.16 ± 0.00
Eicosadienoic acid	C20:2	0.49 ± 0.00	0.42 ± 0.00
Nervonic acid	C24:1 (ω-9)	0.23 ± 0.00	0.26 ± 0.00
Docosahexaenoic acid (DHA)	C22:6 (ω-3)	0.27 ± 0.00	0.28 ± 0.00
Total UFA		**63.60**	**64.64**

***In vitro* anticancer activity on A549 cells**

Cell viability and dose–response analysis

The cytotoxic activity of PMO against A549 human lung adenocarcinoma cells was evaluated by MTT assay following 48 h of treatment at concentrations ranging from 10 to 1,000 µg/mL. As presented in **Table 3** and **Figure 1**, cell viability remained above 60% across all tested concentrations, indicating that PMO did not exert substantial cytotoxic effects within this range.

At the lowest concentrations tested (10 and 50 µg/mL), mean cell viability was 89.12 ± 5.48% and 77.57 ± 6.46%, respectively, consistent with the expectation that low lipid concentrations are insufficient to disrupt cellular homeostasis or trigger metabolic stress in cancer cells. A modest decline in viability was observed at intermediate concentrations (100 - 250

µg/mL), with mean values ranging from approximately 62% to 72%, suggesting a weak onset of cellular response at these doses. At higher concentrations (500 - 1,000 µg/mL), viability appeared to stabilize between 62% and 65%, without further consistent reduction.

Notably, cell viability at 750 µg/mL (68.92 ± 5.79%) was marginally higher than at both 500 µg/mL (64.13 ± 10.17%) and 250 µg/mL (62.46 ± 1.25%), suggesting a non-monotonic dose–response pattern rather than a straightforward linear relationship between concentration and cytotoxicity. This pattern may reflect lipid aggregation at higher concentrations, which can reduce the effective bioavailability of active fatty acid species, or alternatively, a transient activation of cytoprotective mechanisms in response to moderate lipid-induced stress [36]. Increased standard deviation values at 500 - 750 µg/mL further reflect greater inter-replicate variability at these concentrations, likely attributable to minor differences in lipid dispersion and emulsification during sample preparation rather than true biological inconsistency.

One-way ANOVA revealed a statistically significant difference in mean cell viability across concentration groups ($p = 0.001$). Post hoc analysis by Tukey's HSD test indicated that the lowest concentration (10 µg/mL) differed significantly from higher concentrations of 250, 500, 750, and 1,000 µg/mL ($p < 0.05$), whereas no significant pairwise differences were detected among concentrations ≥ 50 µg/mL ($p > 0.05$). This pattern of statistical significance is consistent with the observed plateau in viability above 50 µg/mL and further supports the absence of a dose-dependent cytotoxic response within the tested range. Assay reliability was confirmed by coefficient of variation (CV) values below 15% for most concentration groups, with a small number of groups falling between 15% - 20%, both of which are within the acceptable limits stipulated by the Assay Guidance Manual [37].

Table 3 Viability of A549 cells following treatment with PMO (MTT assay, 48 h).

Concentration (µg/mL)	Cell viability (%)
1,000	63.13 ± 3.43
750	68.92 ± 5.79
500	64.13 ± 10.17
250	62.46 ± 1.25
100	72.14 ± 7.03
50	77.57 ± 6.46
10	89.12 ± 5.48

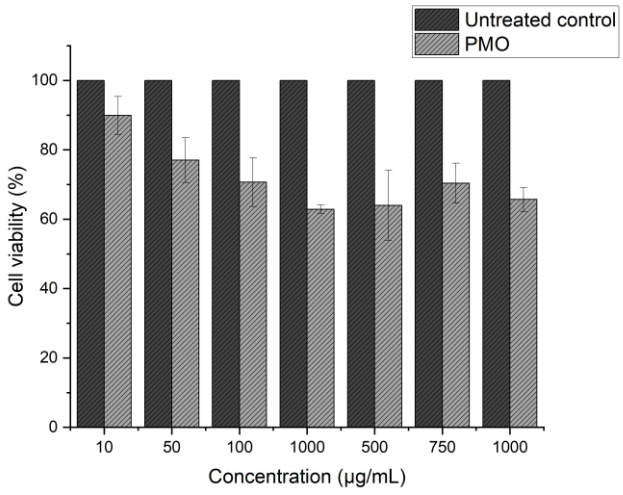


Figure 1 Cell viability of A549 cells treated with different concentrations of PMO compared with untreated control.

IC_{50} estimation

The IC_{50} of PMO against A549 cells was estimated using probit regression analysis following log_{10} transformation of concentration data. As presented in Table 4, individual replicate IC_{50} values were 8,230, 3,450, and 1,880 µg/mL, yielding a mean IC_{50} of 4,520 ± 3,190 µg/mL.

It is important to note that these IC_{50} values were derived through extrapolation beyond the tested concentration range, as 50% inhibition was not achieved at any concentration up to 1,000 µg/mL. Extrapolative IC_{50} values carry inherent uncertainty, as small differences in the slope of the dose–response regression between replicates are substantially amplified during extrapolation, which accounts for the high inter-replicate variability observed (CV = 70.6%). Consequently, the mean IC_{50} of 4,520 µg/mL should be regarded as an approximate estimate rather than a definitive cytotoxic endpoint, and results should be interpreted within this limitation. Extension of the tested concentration range in future studies would be necessary to obtain a reliable IC_{50} by interpolation.

Based on established cytotoxicity classification criteria, compounds with IC_{50} values exceeding 1,000 µg/mL against cancer cell lines are generally considered to have weak or negligible cytotoxic activity [38]. By this criterion, PMO demonstrated weak cytotoxic activity against A549 cells under the conditions applied in this study.

The limited cytotoxic response observed may be partly attributable to the fatty acid composition of PMO, as determined by GC–FID analysis (**Table 2**). PMO was characterized by a predominance of omega-6 linoleic acid (15.21%) and omega-9 oleic acid (44.11%), with relatively low proportions of long-chain omega-3 fatty acids, specifically DHA (0.27%). The balance between omega-6 and omega-3 fatty acids has been recognized as a critical determinant of the pro- or anti-tumorigenic properties of lipid-based compounds. A high omega-6 to omega-3 ratio tends to support a pro-inflammatory cellular environment, as omega-6 fatty acids particularly arachidonic acid serve as substrates for cyclooxygenase (COX) and lipoxygenase (LOX) enzymes, generating pro-tumorigenic eicosanoids including prostaglandin E_2 (PGE_2), which promote cell survival and proliferation rather than apoptosis [39]. In contrast, omega-3 fatty acids such as EPA and DHA have been more consistently associated with antitumor effects through competitive inhibition of eicosanoid synthesis, modulation of PI3K/Akt and NF-κB signaling, and direct induction of apoptosis [40]. The relatively low abundance of these omega-3 species in PMO therefore provides a partial mechanistic explanation for the weak cytotoxic activity observed against A549 cells. Therefore, PMO should not be regarded as a direct anticancer agent but rather as a nutritionally valuable lipid source with limited antiproliferative activity under the experimental conditions evaluated.

Table 4 IC_{50} values of PMO against A549 cells estimated by probit regression.

Replicate	Probit regression equation	IC_{50} (µg/mL)
1	Probit (p) = −1.774 + 0.453 log(C)	8,230
2	Probit (p) = −1.525 + 0.431 log(C)	3,450
3	Probit (p) = −1.482 + 0.453 log(C)	1,880
	Mean ± SD	**4,520 ± 3,190**

***In vitro* anticancer activity against Huh-7 cells**

Cell viability analysis

To further evaluate the biological activity of PMO, cytotoxicity was assessed against Huh-7 human hepatocellular carcinoma cells under the same experimental conditions used for A549 cells. As shown in **Table 5**, Huh-7 cell viability remained stable across all tested PMO concentrations (10 - 1,000 µg/mL), ranging from 97.87 ± 2.99% to 104.60 ± 3.81%, with no apparent dose-dependent response.

Normality testing indicated that at least one group did not satisfy the assumption of normal distribution ($p < 0.05$); therefore, differences among treatment groups were analyzed using the Kruskal–Wallis test. No

statistically significant differences were observed among concentrations ($p = 0.302$), indicating that PMO did not exert a significant cytotoxic effect on Huh-7 cells within the tested concentration range.

Consistent with the results obtained in A549 cells, PMO exhibited negligible cytotoxic activity against Huh-7 cells under the experimental conditions evaluated. These findings suggest that PMO does not possess meaningful direct antiproliferative activity against either cancer cell line tested.

Overall, the *in vitro* results indicate that PMO exhibited negligible cytotoxic activity against both A549 and Huh-7 cell lines. Nevertheless, molecular docking and network pharmacology analyses were subsequently performed as exploratory approaches to investigate potential molecular interactions of the major fatty acid constituents of PMO with cancer-related targets and pathways.

Table 5 Viability of Huh-7 cells following treatment with PMO (MTT assay, 48 h).

Concentration (μg/mL)	Cell viability (%)
1,000	104.60 ± 3.81
750	101.50 ± 1.76
500	99.01 ± 2.81
250	99.23 ± 0.52
100	97.87 ± 2.99
50	103.50 ± 4.69
10	101.30 ± 3.19

Molecular docking

Given the absence of meaningful antiproliferative activity *in vitro*, the computational analyses presented herein should not be interpreted as evidence of anticancer efficacy. Instead, molecular docking and network pharmacology were employed to explore potential interactions between major PMO fatty acids and cancer-related molecular targets, thereby providing hypotheses for future mechanistic investigations.

Rationale for target selection and allosteric site approach

Three proteins central to NSCLC pathogenesis were selected as docking targets in this study: EGFR, mTOR, and MMP-9. EGFR is a receptor tyrosine kinase whose aberrant activation drives tumor cell proliferation and survival in a substantial proportion of NSCLC cases [40]. mTOR functions as a key regulator of cell growth, metabolism, and autophagy, and its hyperactivation is frequently observed in lung cancer through upstream PI3K/Akt signaling [41]. MMP-9 is a zinc-dependent endopeptidase involved in extracellular matrix degradation, tumor invasion, and metastatic progression [42]. Collectively, these 3 targets represent distinct but interconnected nodes in NSCLC biology, making them relevant endpoints for evaluating the multi-target potential of PMO fatty acids.

Molecular docking was performed at allosteric rather than orthosteric (ATP-competitive) binding sites for each target. This decision was guided by 2 considerations. First, the structural characteristics of the fatty acid ligands derived from PMO namely EPA, DHA, ALA, GLA, LA, and OA are long-chain, flexible, and predominantly hydrophobic molecules. These physicochemical features render them more geometrically compatible with the hydrophobic cavities of allosteric sites than with the typically polar and structurally constrained ATP-binding pockets that accommodate planar, rigid inhibitors [43]. Second, allosteric targeting carries particular mechanistic relevance for EGFR, where common resistance-associated mutations including L858R, T790M, and C797S can compromise the efficacy of competitive active-site inhibitors. Allosteric modulation of EGFR may stabilize the inactive kinase conformation independently of the mutational status of the ATP-binding site, offering a mechanistic rationale for exploring this approach with lipid-derived.

Docking validation

Prior to docking of PMO fatty acids, the reliability of the docking protocol was assessed by redocking the co-crystallized native ligand of each target protein into its original binding site. The resulting RMSD values were 1.049 Å for EGFR, 1.452 Å for mTOR, and 0.896 Å for MMP-9, all below the accepted threshold of 2.0 Å. These values indicate that the docking protocol successfully reproduced the experimentally observed binding poses of the native ligands, confirming its suitability for subsequent docking of PMO fatty acid compounds.

Binding affinity analysis

The binding affinity values of PMO fatty acids against all 3 target proteins are summarized in **Table 6**, alongside the corresponding native ligand affinities for reference. As shown in **Table 6**, all PMO fatty acids exhibited lower binding affinities than the respective native ligands against all 3 target proteins, which is expected given the structural differences between the fatty acid ligands and the purpose-designed synthetic inhibitors used as reference compounds. The binding affinity values of PMO fatty acids ranged from −6.03 to −7.41 kcal/mol across all target–ligand combinations, indicating the capacity to form moderately stable interactions at the allosteric sites, though with weaker affinity than the native ligands.

Among all fatty acids evaluated, DHA consistently produced the highest binding affinity against all 3 targets: −7.30 kcal/mol for EGFR, −7.41 kcal/mol for mTOR, and −6.92 kcal/mol for MMP-9. This pattern is consistent with previous molecular docking studies reporting that long-chain polyunsaturated omega-3 fatty acids, particularly DHA, tend to demonstrate stronger interactions with kinase and protease targets than shorter-chain or more saturated fatty acid species, which has been attributed to the greater number of rotatable double bonds enabling more favorable conformational adaptation within hydrophobic binding cavities [44]. GLA ranked second for EGFR (−6.98 kcal/mol), while ALA showed the second-highest affinity for MMP-9 (−6.54 kcal/mol), suggesting that the degree and positional pattern of unsaturation influence binding behavior in a target-dependent manner.

The binding affinities observed in this study are broadly comparable to values reported for other natural lipid-derived compounds docked against EGFR and mTOR allosteric sites, where affinities in the range of −6.0 to −8.0 kcal/mol have been reported for fatty acids and related bioactive lipids. Although these affinities are substantially weaker than those of clinical kinase inhibitors, they are within a range considered sufficient for moderate non-covalent interactions and are consistent with the biological activity profile expected of dietary lipid compounds acting as modulatory rather than inhibitory agents.

Protein–ligand interaction analysis

The interaction profiles of the best-performing fatty acid against each target protein were analyzed in detail using 2-dimensional (2D) and 3-dimensional (3D) visualization (**Figures 2 - 7**). The selection of the representative pose for each ligand was based not solely on the lowest binding energy value, but on the combination of energetic stability and interaction pattern similarity to the native ligand — specifically, the number of shared key residues and the nature of the interactions observed at the allosteric binding site.

At the allosteric site of EGFR, the fatty acids EPA, DHA, GLA, LA, and OA formed hydrogen bond interactions with Asp-855, a residue located within the DFG motif of the kinase activation loop (**Figures 2**). At the FKBP12-rapamycin binding (FRB) domain allosteric site of mTOR, ALA, GLA, and OA formed hydrogen bond interactions with Arg-73, alongside hydrophobic contacts with Phe-77 and Phe-2108 (**Figures 6**). EPA, DHA, and LA interacted primarily through hydrophobic contacts at the same site, without forming hydrogen bonds with Arg-73 under the docking conditions applied. The FRB domain is the binding site of rapamycin and represents a well-characterized allosteric regulatory region of mTOR; ligand binding at this site has been associated with disruption of mTOR complex assembly and downstream signaling attenuation. DHA achieved the highest binding affinity at this target (−7.41 kcal/mol) despite the absence of a hydrogen bond with Arg-73, suggesting that the extended hydrophobic surface area of its polyunsaturated chain contributes substantially to binding stability through van der Waals and

hydrophobic interactions with Phe-77 and Phe-2108 (**Figure 5**).

At the allosteric site of MMP-9, all PMO fatty acids interacted primarily through hydrophobic contacts at Val-101 and Tyr-179 (**Figures 6**). These residues are located within the allosteric pocket of pro-MMP-9, a site distinct from the catalytic zinc-binding domain. Ligand placement at this pocket has been proposed to stabilize the pro-domain inhibitory segment, potentially limiting the proteolytic activation of MMP-9 and thereby reducing its capacity to degrade extracellular matrix components involved in tumor invasion and metastasis [23]. The absence of hydrogen bond interactions at this site for most fatty acids is consistent with the predominantly hydrophobic character of the MMP-9 allosteric pocket, which lacks the polar residues typically involved in hydrogen bonding with ligands at the catalytic site. DHA again produced the highest binding affinity at MMP-9 (−6.92 kcal/mol) (**Figure 7**), followed by ALA (−6.54 kcal/mol).

Table 6 Binding affinity values (kcal/mol) and RMSD of PMO fatty acids docked against NSCLC-related target proteins.

Protein	RMSD	Ligand	Binding Affinity
EGFR (PDB ID: 5D41)	1,049 A	57N	−9.30
		EPA	−6.89
		DHA	**−7.30**
		ALA	−6.78
		GLA	−6.98
		LA	−6.90
		OA	−6.66
mTOR (PDB ID: 4DRI)	1,452 A	RAP	−19.16
		EPA	−6.39
		DHA	**−7.41**
		ALA	−6.56
		GLA	−6.48
		LA	−6.41
		OA	−6.57
MMP9 (PDB ID: 5UE4)	0,896 A	5XQ	−8.10
		EPA	−6.16
		DHA	**−6.92**
		ALA	−6.54
		GLA	−6.33
		LA	−6.12
		OA	−6.03

The interactions between amino acid residues and the fatty acid ligands exhibiting the highest binding affinities are presented in the corresponding 2D and 3D visualizations. The best binding affinity in the analysis of ligand-protein interactions is not only determined by the lowest bond energy value but also considered based on the suitability of the amino acid interaction pattern with the natural ligand in each protein. The compound pose is selected as the most representative if it can interact with a greater number of key residues and shows similarities in the type of interaction and residues similar to natural ligands at the protein binding site. This analysis is performed to ensure that fatty acid compounds are not only energetically stable but also relevant to the binding mechanism in the target protein. The 3-dimensional and 2-dimensional visualizations of protein-ligand interactions are shown in the figures below.

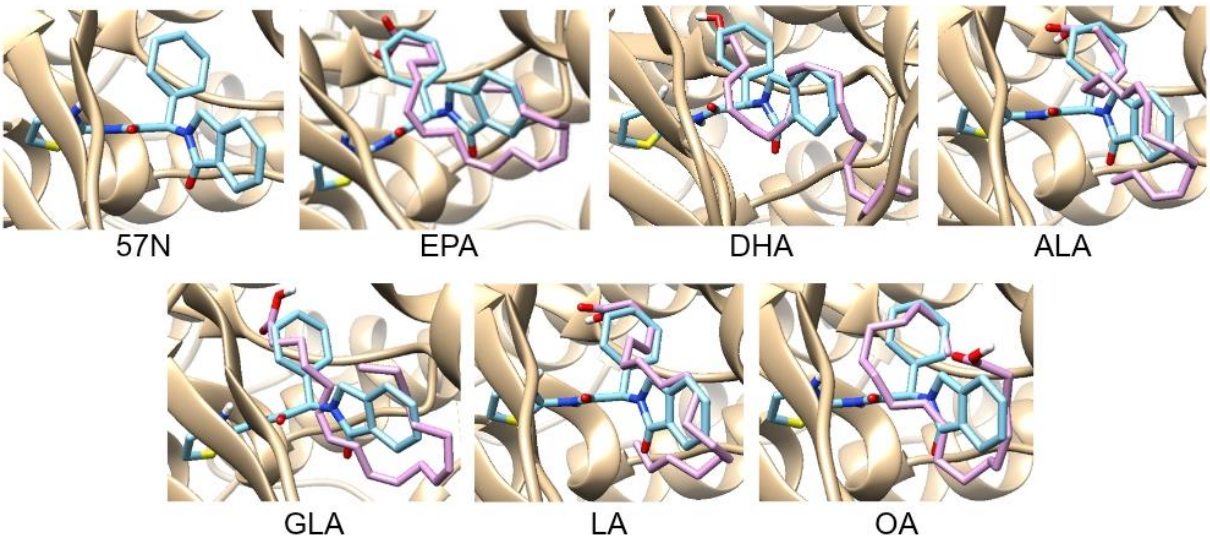


Figure 2 3D Interaction of ligand-protein compounds of PMO fatty acids on EGFR (PDB ID: 5D41).

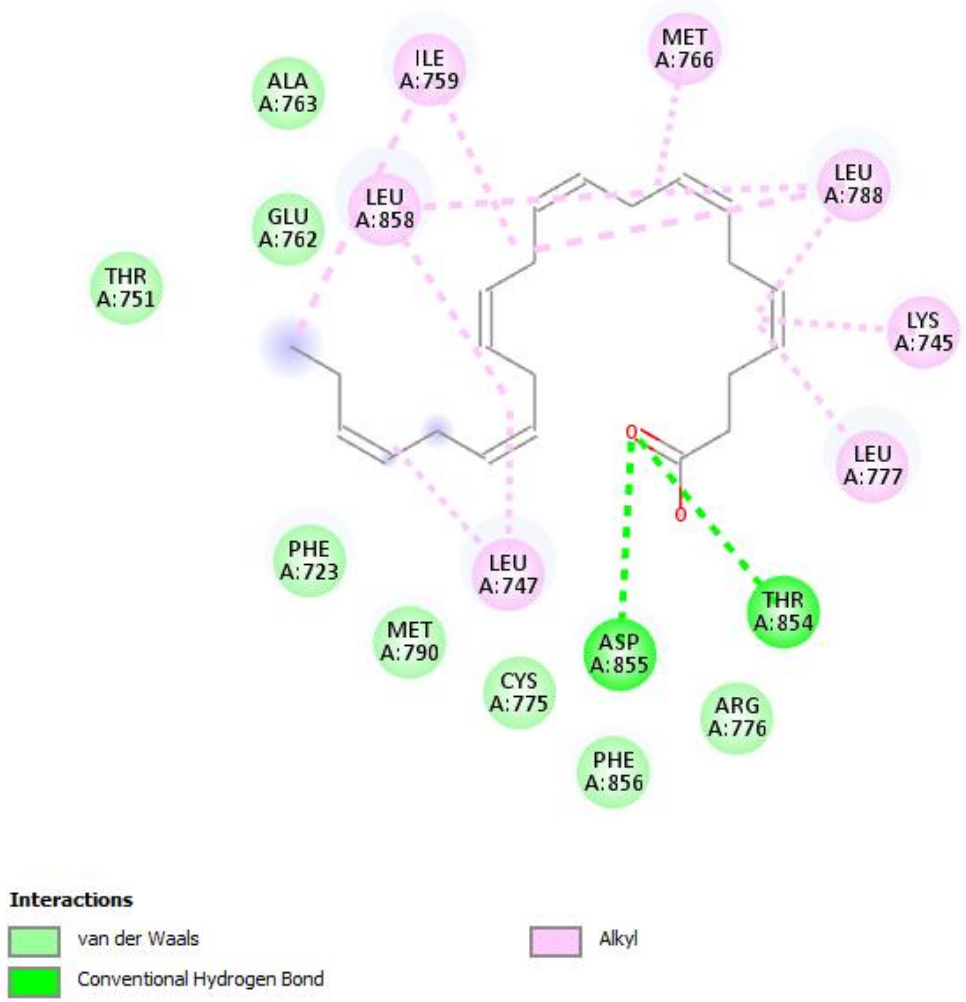


Figure 3 2D Interaction of ligand-protein compounds of DHA on EGFR (PDB ID: 5D41).

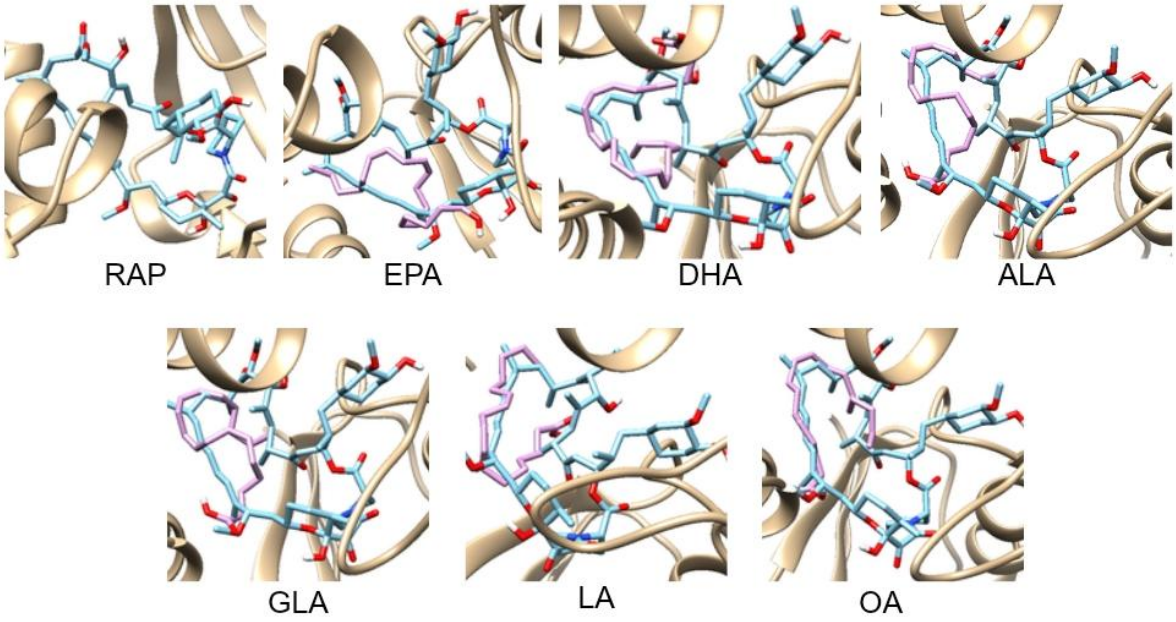


Figure 4 3D Interaction of ligand-protein compounds of PMO fatty acids on mTOR (PDB ID: 4DRI).

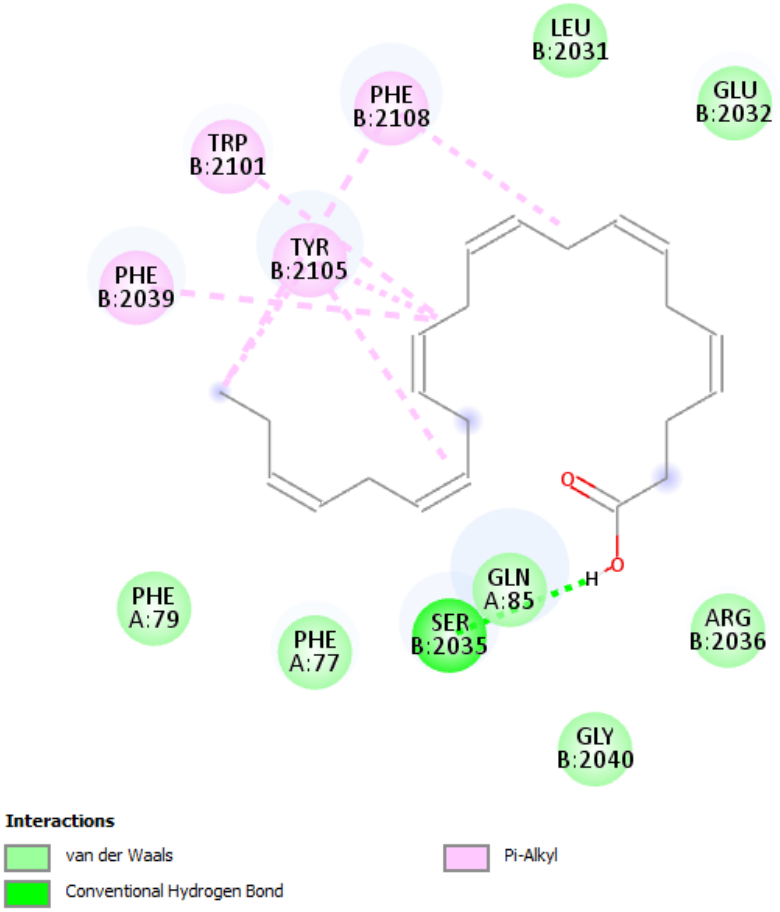


Figure 5 2D interaction of ligand-protein compounds of DHA on mTOR (PDB ID: 4DRI).

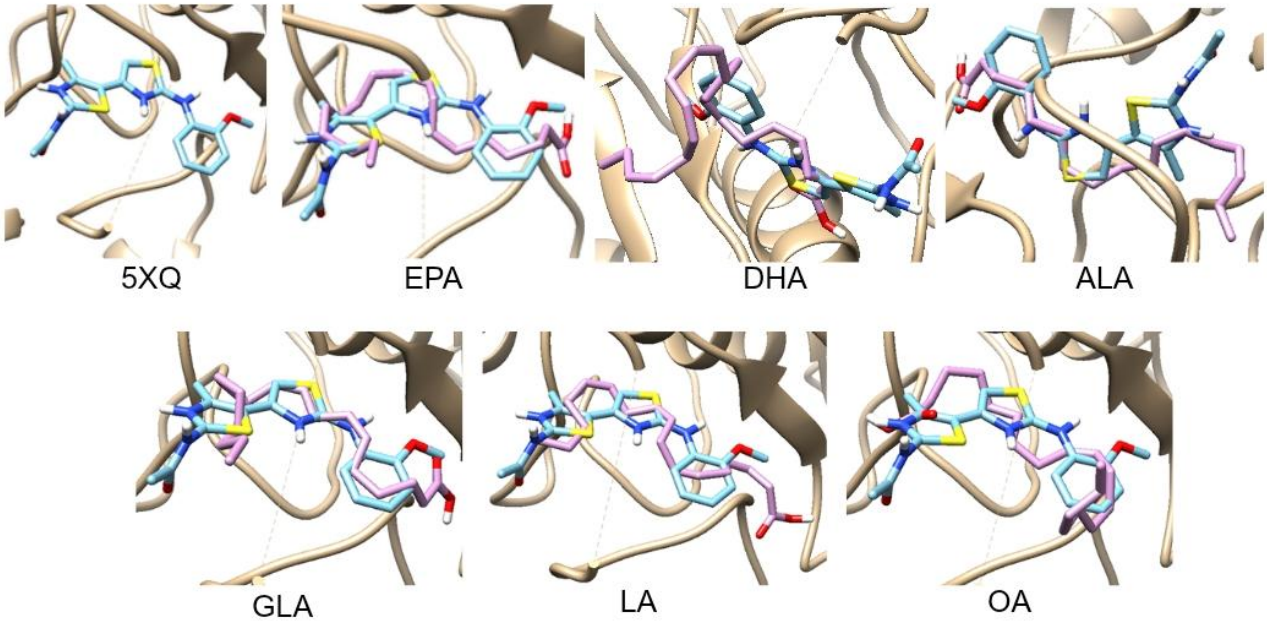


Figure 6 3D Interaction of ligand-protein compounds of PMO fatty acids on MMP9 (PDB ID: 5UE4).

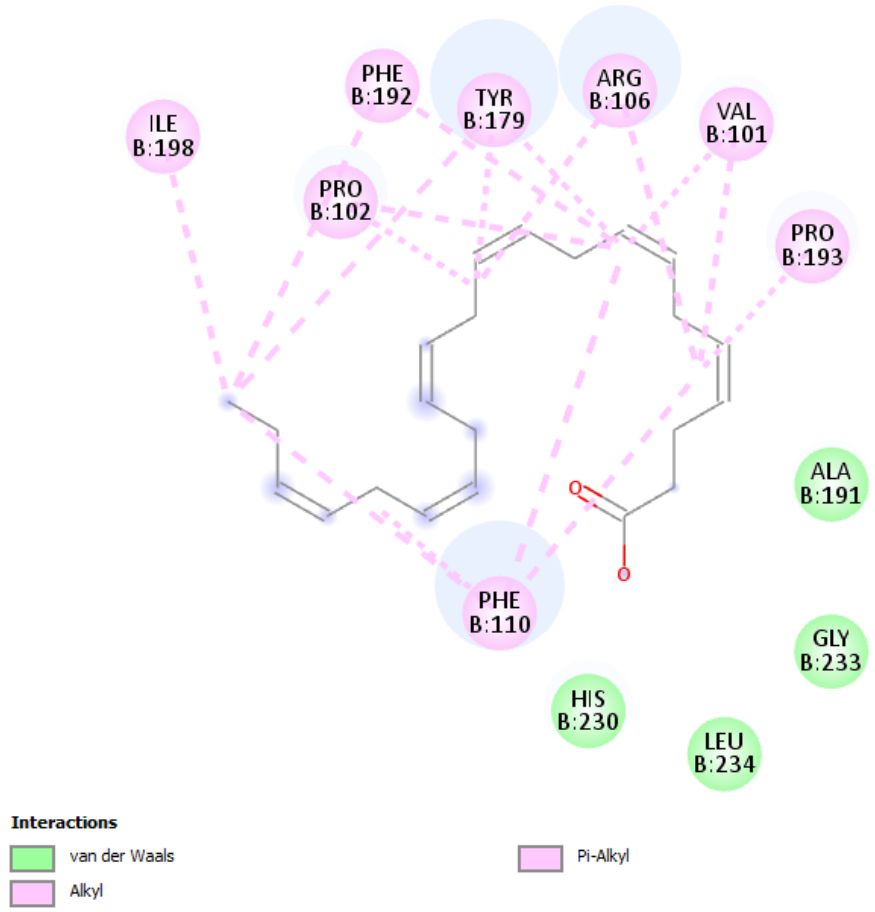


Figure 7 2D Interaction of ligand-protein compounds of PMO fatty acids on MMP9 (PDB ID: 5UE4).

The molecular docking results were consistent with the *in vitro* cytotoxicity findings, which demonstrated weak anticancer activity of PMO against both A549 and Huh-7 cancer cells. Among the major fatty acids identified, DHA exhibited the strongest binding affinity toward the selected cancer-related targets, suggesting a greater potential contribution to anticancer activity compared with the other fatty acids evaluated. However, GC–FID analysis revealed that DHA was present only in a very low proportion (0.27% - 0.28% of total fatty acids) in PMO. Consequently, the overall biological activity of the oil is likely limited by the low abundance of this bioactive omega-3 fatty acid. In contrast, PMO was predominantly composed of oleic acid and linoleic acid, which generally exhibit weaker interactions with cancer-associated molecular targets than DHA. Therefore, the low DHA content may partially explain the weak cytotoxic effects observed in the *in vitro* assays, despite the favorable docking performance of DHA as an individual compound.

Network pharmacology

The PPI results show the top 10 proteins related to NSCLC (**Figure 8**), with the highest degree shown in the darker, larger node. MDM2 was identified as the hub protein with the highest degree, followed by other proteins in this study. This finding indicates that MDM2 participates in extensive protein–protein interactions and may serve as a key regulator within biological networks and the pathogenesis of disease [45, 46]. MDM2 is an oncogenic protein that is frequently overexpressed across a wide range of human cancers. It functions as a principal negative regulator of the tumor suppressor p53 by promoting its ubiquitination, proteasomal degradation, and nuclear export, thereby suppressing apoptosis and facilitating tumor cell proliferation [47, 48]. PTGS2 plays a key role in inflammation-driven tumor progression in NSCLC. Its overexpression during chronic inflammation promotes the production of prostaglandins, leading to increased reactive oxygen species (ROS) that induce DNA damage and genomic instability. At the same time, PTGS2 activates signaling pathways that enhance cell proliferation and survival. Thus, persistent PTGS2 activity links chronic inflammation to elevated DNA damage and accelerated cell division in lung tissues [49, 50].

Other proteins identified in the PPI network, such as CASP8, CDK1, and several others, are also associated with cancer through distinct molecular mechanisms. For instance, CDK1 functions as a key regulator of mitosis; its overactivation can lead to uncontrolled cellular proliferation. In addition, previous bioinformatics studies have consistently identified CDK1 as a common node in network analysis, suggesting its significant regulatory role in NSCLC [54-53]. CASP8 has been identified as a key node in the protein–protein interaction network, suggesting its central role in NSCLC pathogenesis. Previous studies have reported a high frequency of genetic alterations, including polymorphisms, in CASP8 among NSCLC patients. Functionally, CASP8 is a critical regulator of apoptosis, and its downregulation has been strongly associated with chemoresistance. These findings indicate that CASP8 may contribute to tumor progression by evading apoptosis and highlight its potential as a therapeutic target in NSCLC [54].

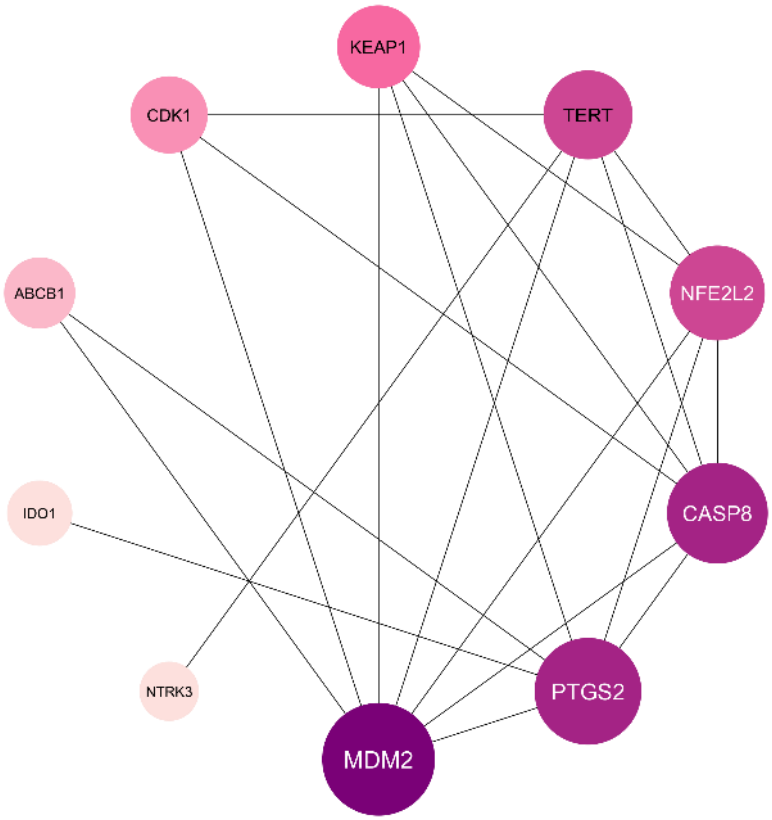
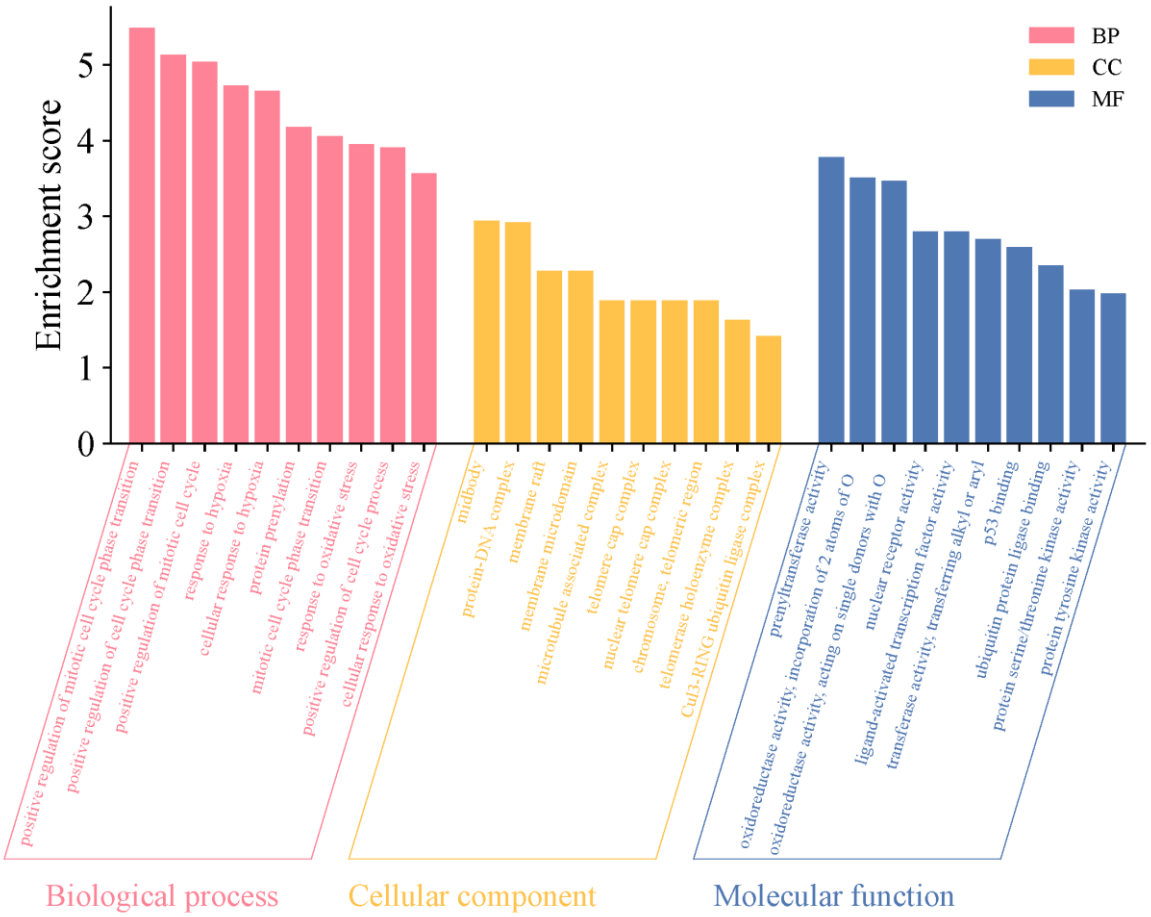


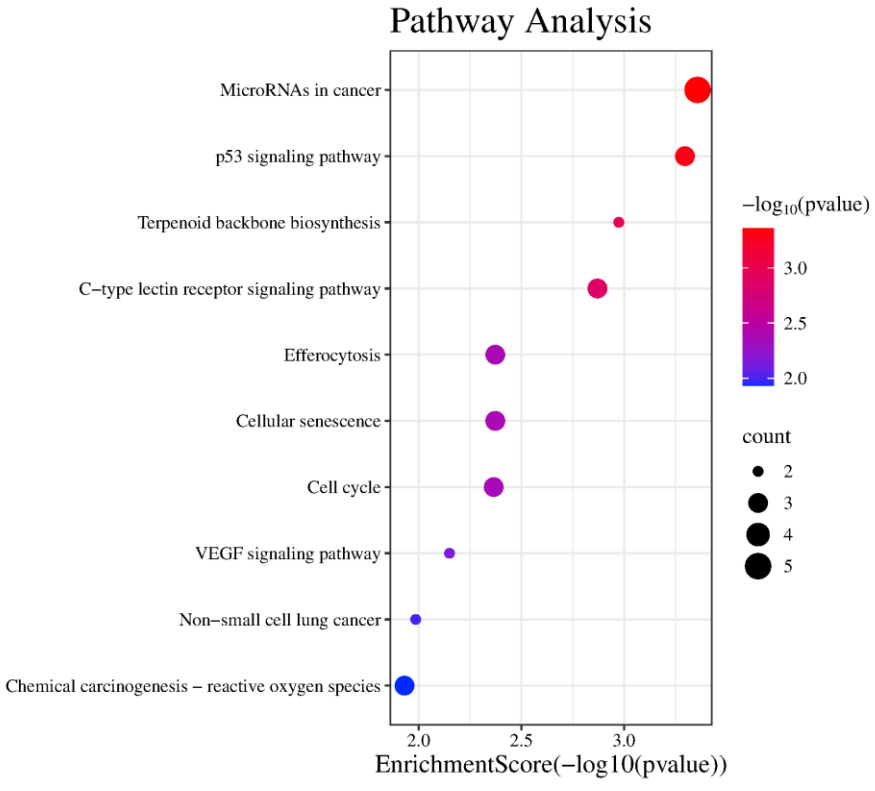
Figure 8 Protein-protein interaction of fatty acids and NSCLC.

The integrated Gene Ontology (GO) and Kyoto Encyclopedia of Genes and Genomes (KEGG) pathway enrichment analyses (**Figure 9**) reveal a clear and biologically coherent picture: The input gene set is strongly linked to several fundamental processes that drive NSCLC. In the biological process (BP) category, the most prominent enrichments involve positive regulation of mitotic cell-cycle phase transition, response to hypoxia, and response to oxidative stress. These findings make intuitive sense in the context of NSCLC, where tumors must proliferate rapidly, adapt to low-oxygen environments, and withstand chronic oxidative damage [55,56]. The cellular component (CC) results reinforce this story, showing enrichment in telomere cap complexes, microtubule-associated structures, membrane rafts, and the Cul3-RING ubiquitin ligase complex, features that support replicative immortality, efficient cell division, and KEAP1/NRF2-mediated stress resistance, all of which are well-documented in lung adenocarcinoma. On the molecular function (MF) side, the standout terms prenyltransferase activity and p53 binding point directly to KRAS activation via farnesylation and the disruption of p53 tumor-suppressor pathways, two classic alterations in NSCLC [57].

These GO insights are nicely complemented by the KEGG pathway analysis, which identified the "Non-small cell lung cancer" pathway itself, along with p53 signaling, microRNAs in cancer, cellular senescence, VEGF signaling, and terpenoid backbone biosynthesis. The latter is especially relevant, as it provides the precursors needed for KRAS prenylation, a key oncogenic event in many lung tumors [58]. Taken together, the results portray a molecular landscape in which the queried genes promote unchecked cell-cycle progression, help cells evade senescence, resist oxidative stress through the KEAP1/NFE2L2 axis, maintain telomeres, and sustain angiogenesis and survival signaling. This integrated profile not only confirms the strong relevance of the gene set to NSCLC but also highlights potential therapeutic entry points for targeted intervention.



(A)



(B)

Figure 9 Gene ontology (A) and KEGG pathways enrichment analysis (B).

The merged compound-target network was constructed using Cytoscape to visualize the multi-target interactions between 7 major fatty acids identified in PMO and 28 high-degree protein targets associated with NSCLC. The central rectangular nodes (orange-to-yellow gradient) represent the top-ranked NSCLC-related proteins, including MAP2K2, PIN1, MDM2, FNTA, PTGER4, CDK1, PREP, PTGS2, FNTB, KEAP1, TERT, NFE2L2, CDC25B, ABCB1, IDO1, CASP8, TOP1, RXRG, NTRK3, RORC, and MME. These targets are surrounded by seven peripheral red circular nodes representing the fatty acids: elaidic acid, palmitoleic acid, palmitic acid, myristic acid, α-linolenic acid, and linoleic acid. Each fatty acid node connects to multiple central targets, illustrating the polypharmacological potential of the oil's lipid components.

This network topology directly reflects key mechanistic drivers of NSCLC (**Figure 10**). The enrichment of cell-cycle regulators (CDK1, CDC25B, PIN1) underscores uncontrolled G2/M-phase progression, a hallmark of rapid tumor proliferation [59,60]. Telomerase reverse transcriptase (TERT) highlights replicative immortality, while the KEAP1/NFE2L2 axis points to constitutive activation of the NRF2 pathway, enabling cancer cells to survive chronic oxidative stress and hypoxia within the lung tumor microenvironment [61,62]. KRAS prenylation enzymes (FNTA/FNTB) are critical for membrane anchoring and oncogenic signaling in approximately more than 10% of NSCLC cases, particularly adenocarcinomas [61,66]. Concurrently, MDM2 and CASP8 modulation suggest disruption of p53-mediated apoptosis and evasion of programmed cell death [62,63], whereas ABCB1 indicates potential contributions to multidrug resistance [64]. Inflammatory mediators (PTGS2/COX-2, PTGER4) further link the network to immune evasion [65] Collectively, the fatty acids in Pangasius catfish oil appear capable of modulating these interconnected NSCLC pathways, including cell-cycle deregulation, oxidative stress resistance, telomere maintenance, KRAS activation, and apoptosis resistance, positioning the oil as a promising multi-target natural agent for complementary NSCLC therapy.

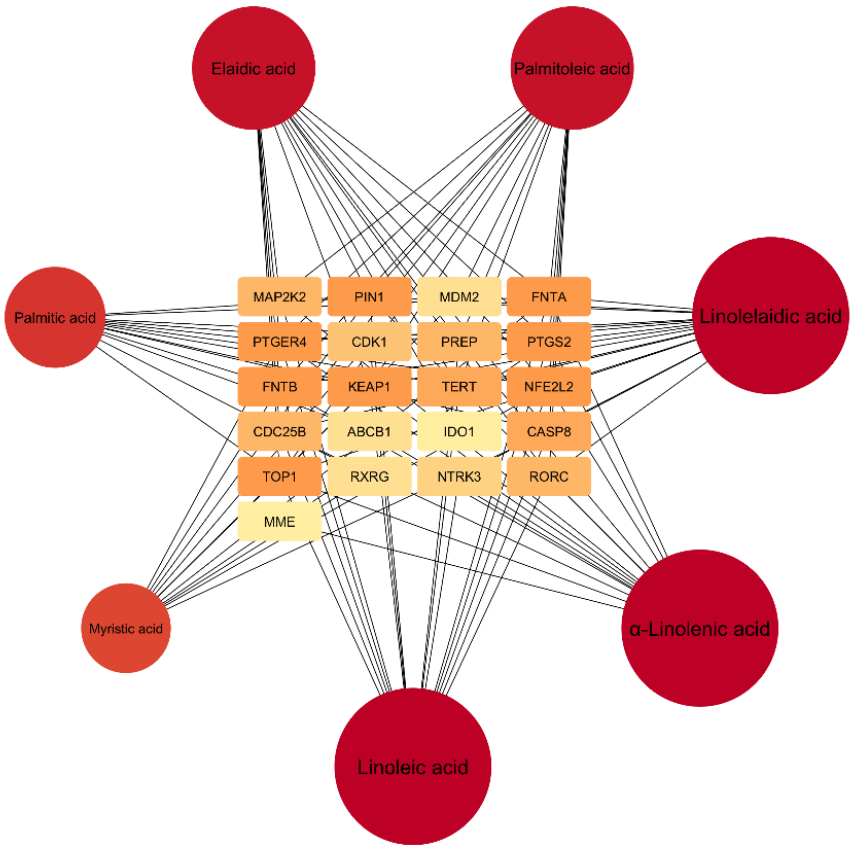


Figure 10 Network construction of fatty acids and NSCLC target.

Although the computational analyses identified several cancer-related targets, including EGFR, mTOR, and MMP-9, these predicted interactions did not translate into measurable antiproliferative effects in the present *in vitro* experiments. Therefore, the docking and network pharmacology findings should be regarded as hypothesis-generating rather than confirmatory evidence of anticancer activity.

Conclusions

This study comprehensively evaluated the physicochemical properties, fatty acid composition, and biological activity of PMO obtained by mechanical pressing and Soxhlet extraction. Soxhlet extraction provided a higher oil yield, whereas mechanically pressed oil exhibited more favorable physicochemical quality, as reflected by lower acid and peroxide values, higher saponification value, and slightly higher iodine value. Despite differences in extraction performance, both methods produced oils with highly similar fatty acid profiles, characterized by a predominance of unsaturated fatty acids, particularly oleic and linoleic acids.

In vitro evaluation demonstrated negligible cytotoxic activity of PMO against both A549 and Huh-7 cancer cell lines under the experimental conditions tested, indicating that PMO should not be considered a direct anticancer agent. Although molecular docking and network pharmacology analyses identified potential interactions between major PMO fatty acids and several cancer-related targets, including EGFR, mTOR, and MMP-9, these computational findings were not supported by significant antiproliferative activity *in vitro* and should therefore be regarded as exploratory rather than confirmatory evidence of anticancer activity.

Overall, the results indicate that the extraction method has a greater impact on oil yield and physicochemical quality than on fatty acid composition or biological activity. Mechanical pressing represents a promising solvent-free approach for producing PMO with favorable quality characteristics. Future studies should focus on comprehensive lipidomic characterization, oxidative stability, and other biological or nutritional properties to further explore the potential applications of this freshwater fish oil.

Acknowledgements

The authors gratefully acknowledge financial support from the Directorate of Research and Community Service (DRPM), Universitas Brawijaya, through the *Penelitian Dasar Unggulan* scheme, under contract number 01046.1/UN10.A0501/B/KS/2025. The authors also sincerely thank the Tropical Disease Laboratory, Universitas Airlangga, Indonesia for providing facilities and technical support for the anticancer experiments conducted in this study.

CRediT author statement

Anggita Rosiana Putri: Conceptualization; Methodology; Funding acquisition; Project administration; Supervision; Data interpretation; Writing - Original Draft; Writing - Review & Editing. **Nathaniel Indra Hentyan**: Investigation; Formal analysis; Data curation; Visualization; Writing - Original Draft. **Risma Ainun Nisa**: Investigation; Data curation; Validation. **Salma Izzah Abidah**: Investigation; Data curation; Validation. **Luthfi Ahmad Muchlashi**: Methodology; Software; Formal analysis; Writing - Review & Editing. **Prisma Trida Hardani**: Investigation; Resources; Validation. **Kevin Awidarta:** Software; Formal analysis; Visualization. **Leena Suntornsuk**: Methodology; Supervision; Validation; Writing - Review & Editing.

References

[1] AG Jayathilake, RB Luwor, K Nurgali and XQ Su. Molecular mechanisms associated with the inhibitory role of long chain n-3 PUFA in colorectal cancer. *Integrative Cancer Therapies* 2024. https://doi.org/10.1177/15347354241243024

[2] R Ashraf, CDC Buchanan, LM Hillyer, E Ogloblina, GA Wood, RP Bazinet, S Subedi, AM Edwards, YI Kim, WJ Muller, JM Monk, LE Robinson and DWL Ma. Lifelong n-3 PUFA consumption reduces HER2+ mammary tumour growth and alters immune markers compared to safflower- or corn oil-based sources of n-6 PUFA. *Nutrients* 2026; **18(4)**, 606.

[3] J de Freitas Rodrigues, HK Philippsen, MF Dolabela, CY Nagamachi and JC Pieczarka. The

potential of DHA as cancer therapy strategies: A narrative review of *in vitro* cytotoxicity trials. *Nutrients* 2023; **15(8)**, 2006.

[4] Y Yin, C Sui, F Meng, P Ma and Y Jiang. The omega-3 polyunsaturated fatty acid docosahexaenoic acid inhibits proliferation and progression of non-small cell lung cancer cells through the reactive oxygen species-mediated inactivation of the PI3K/Akt pathway. *Lipids in Health and Disease* 2017; **16(1)**, 87.

[5] RB Hashim, EF Jamil, FH Zulkipli and JM Daud. Fatty acid compositions of silver catfish, *Pangasius sp.* farmed in several rivers of Pahang, Malaysia. *Journal of Oleo Science* 2015; **64(2)**, 205-209.

[6] AR Putri, A Rohman and S Riyanto. Authentication of patin (*Pangasius micronemus*) fish oil adulterated with palm oil using FTIR spectroscopy combined with chemometrics. *International Journal of Applied Pharmaceutics* 2019; **11(3)**, 195-199.

[7] AR Putri, A Rohman and S Riyanto. Comparative study of fatty acid profiles in patin (*Pangasius micronemus*) and gabus (*Channa striata*) fish oil and its authentication using FTIR spectroscopy combined with chemometrics. *International Journal of Applied Pharmaceutics* 2019; **11(6)**, 55-60.

[8] D D'Eliseo and F Velotti. Omega-3 fatty acids and cancer cell cytotoxicity: Implications for multi-targeted cancer therapy. *Journal of Clinical Medicine* 2016; **5(2)**, 15.

[9] H Sung, J Ferlay, RL Siegel, M Laversanne, I Soerjomataram, A Jemal and F Bray. Global cancer statistics 2020: GLOBOCAN estimates of incidence and mortality worldwide for 36 cancers in 185 countries. *CA: A Cancer Journal for Clinicians* 2021; **71(3)**, 209-249.

[10] A Zhang, K Miao, H Sun and CX Deng. Tumor heterogeneity reshapes the tumor microenvironment to influence drug resistance. *International Journal of Biological Sciences* 2022; **18(7)**, 3019-3033.

[11] ZF Lim and PC Ma. Emerging insights of tumor heterogeneity and drug resistance mechanisms in lung cancer targeted therapy. *Journal of Hematology and Oncology* 2019; **12(1)**, 134.

[12] N Rahman, S Hashem, S Akther and JS Jothi. Impact of various extraction methods on fatty acid profile, physicochemical properties, and nutritional quality index of Pangus fish oil. *Food Science and Nutrition* 2023; **11(8)**, 4688-4699.

[13] E Kalkan, HK Cavdar and M Maskan. Health impacts and innovative extraction methods of fish oil: A review. *European Journal of Lipid Science and Technology* 2025; **127(2)**, e202400171.

[14] J Chen and H Liu. Nutritional indices for assessing fatty acids: A mini-review. *International Journal of Molecular Sciences* 2020; **21(16)**, 5695.

[15] D Lv, R Wang, M Chen, Y Li and C Cao. Fish intake, dietary polyunsaturated fatty acids, and lung cancer: Systematic review and dose-response meta-analysis of 1.7 million men and women. *Nutrition and Cancer* 2022; **74(6)**, 1976-1985.

[16] E Patterson, R Wall, GF Fitzgerald, RP Ross and C Stanton. Health implications of high dietary omega-6 polyunsaturated fatty acids. *Journal of Nutrition and Metabolism* 2012; **2012**, 539426.

[17] A Swaidan, F Grasso, F Falco, F Turrini and R Boggia. Advances in fish oil extraction and enrichment: A comprehensive review of conventional and green technologies for high-quality omega-3-rich oil production. *Sustainable Food Technology* 2026. https://doi.org/10.1039/D5FB00888C

[18] KR Pawar and PK Nema. Apricot kernel characterization, oil extraction, and its utilization: A review. *Food Science and Biotechnology* 2023; **32(3)**, 249-263.

[19] Z Shahzadi, Z Yousaf, I Anjum, M Bilal, H Yasin, A Aftab, A Booker, R Ullah and A Bari. Network pharmacology and molecular docking: Combined computational approaches to explore the antihypertensive potential of Fabaceae species. *Bioresources and Bioprocessing* 2024; **11(1)**, 53.

[20] SS Hassanein, AL Abdel-Mawgood and SA Ibrahim. EGFR-dependent extracellular matrix protein interactions might light a candle in cell behavior of non-small cell lung cancer. *Frontiers in Oncology* 2021; **11**, 766659.

[21] AOAC International. *AOAC official method 940.28: Fatty acids (free) in crude and refined oils.* Oxford University Press, New York, 2023.

[22] AOAC International. *Official methods of analysis.* 18th ed. AOAC International, Gaithersburg, United States, 2005.

[23] Y Lima-Pereira, EMO de Souza, DS dos Reis, IGC Barcellos-Silva, KSL Miki, VF Veiga-Júnior and BE Teixeira-Costa. Current perspectives on the extraction, isolation, and identification of fats and fatty acids using conventional and green methods. *Separations* 2025; **12(6)**, 160.

[24] DN Hagbe, FFD Dongmo, ARF Mba, FHN Ngamga, BS Noutsa, LL Lienou, RME Etame and I Gouado. Comparative study of extraction methods for nutritional and safety assessment of fish oils from *Heterotis niloticus* co-products. *Applied Food Research* 2025; **5(1)**, 100783.

[25] A Akhmedov, N Erkaeva and O Rakhmonkulova. New technology for primary purification of sunflower and soybean oils. *E3S Web of Conferences* 2023; **401**, 04034.

[26] S Wang, J Wang, G Dong, X Chen, S Lei and Q Bai. Effect of different extraction methods on quality characteristics of rapeseed and flaxseed oils. *Journal of Food Quality* 2022; **2022**, 8296212.

[27] Y Elouafy, A El Yadini, H El Moudden, H Harhar, MM Alshahrani, AA Al Awadh, KW Goh, LC Ming, A Bouyahya and M Tabyaoui. Influence of the extraction method on the quality and chemical composition of walnut (*Juglans regia* L.) oil. *Molecules* 2022; **27(22)**, 7681.

[28] CODEX Alimentarius. *Standard for fish oils CXS 329-2017.* FAO/WHO Codex Alimentarius Commission, Rome, Italy, 2024.

[29] T Dedebas. Oxidative stability of poppy seed oils: Kinetic and thermodynamic analyses under accelerated conditions. *Journal of Food Measurement and Characterization* 2024; **18(3)**, 1969-1979.

[30] M Ivanova, A Hanganu, R Dumitriu, M Tociu, G Ivanov, C Stavarache, L Popescu, A Ghendov-Mosanu, R Sturza, C Deleanu and NA Chira. Saponification value of fats and oils as determined from ^{1}H-NMR data: The case of dairy fats. *Foods* 2022; **11(10)**, 1466.

[31] AA Ayeloja, WA Jimoh and TV Oyewole. Nutritional quality of fish oil extracted from selected marine fish species. *Food and Humanity* 2024; **2**, 100212.

[32] MM Roman-Lara, KJ Chong, RM Bill and AD Goddard. A miniaturized iodine value assay for quantifying the unsaturated fatty acid content of lipids, lipid mixtures, and biological membranes. *Lipids* 2025; **60(4)**, 201-210.

[33] United States Pharmacopeia. *US Pharmacopeia*. United States Pharmacopeial Convention, Rockville, United States, 2026.

[34] PW Harlina, AY Nasution, I Musfiroh, M Muchtaridi, F Geng, T Yuliana and VP Yarlina. A sustainable source of freshwater fish oil: Nutritional and functional insights through lipidomics and metabolomics. *LWT* 2026; **241**, 119046.

[35] AR Putri, W Setyaningsih, MP Lovillo, CAC Fernández, A Rohman, S Riyanto and YP Jang. Ultrasound-assisted extraction of patin fish oil: optimization using response surface methodology–Box Behnken design. *Indonesian Journal of Chemistry* 2025; **25(5)**, 1462-1474.

[36] SS Borges, SEM Miranda, VHS Marinho, ALB de Barros, S Yoshioka, LIS Hage-Melim, ACJ Silva, IM Ferreira and AEMFMO Oliveira. Evaluation of the cytotoxic activity of nanostructured lipid carrier systems for fatty acid amides and silk fibroins in breast cancer cell lines. *Molecules* 2025; **30(16)**, 3337.

[37] CJ Briscoe, MR Stiles and DS Hage. System suitability in bioanalytical LC/MS/MS. *Journal of Pharmaceutical and Biomedical Analysis* 2007; **44(2)**, 484-491.

[38] ML Nordin, A Abdul Kadir, ZA Zakaria, R Abdullah and MNH Abdullah. *In vitro* investigation of cytotoxic and antioxidative activities of Ardisia crispa against breast cancer cell lines, MCF-7 and MDA-MB-231. *BMC Complementary and Alternative Medicine* 2018; **18(1)**, 87.

[39] E Kaviani, F Hajibabaie, N Abedpoor and K Safavi. Synergic effects and possible mechanism of omega-6 fatty acids (ω-6) on immune system, inflammation, and cancer. *Molecular Nutrition and Food Research* 2025; **69(12)**, e70092.

[40] PC Hsu, DM Jablons, CT Yang and L You. Epidermal growth factor receptor (EGFR)

pathway, yes-associated protein (YAP) and the regulation of programmed death-ligand 1 (PD-L1) in non-small cell lung cancer (NSCLC). *International Journal of Molecular Sciences* 2019; **20(15)**, 3821.

[41] RA Saxton and DM Sabatini. mTOR signaling in growth, metabolism, and disease. *Cell* 2017; **168(6)**, 960-976.

[42] M Wolosowicz, S Prokopiuk and TW Kaminski. Matrix metalloproteinase-9 (MMP-9) as a therapeutic target: Insights into molecular pathways and clinical applications. *Pharmaceutics* 2025; **17(11)**, 1425.

[43] C Kousparou, M Fyrilla, A Stephanou and I Patrikios. DHA/EPA (omega-3) and LA/GLA (omega-6) as bioactive molecules in neurodegenerative diseases. *International Journal of Molecular Sciences* 2023; **24(13)**, 10717.

[44] D Tocher, M Betancor, M Sprague, RE Olsen and JA Napier. Omega-3 long-chain polyunsaturated fatty acids, EPA and DHA: Bridging the gap between supply and demand. *Nutrients* 2019; **11(1)**, 89.

[45] Z Ma, A Ajibade and X Zou. Docking strategies for predicting protein-ligand interactions and their application to structure-based drug design. *Communications in Information and Systems* 2024; **24(3)**, 199-230.

[46] Y Chen, Y Sun, Y Ding, Y Ding, S Liu, X Zhou, H Wu, J Xiao and B Lu. Recent progress in fish oil-based emulsions by various food-grade stabilizers: Fabrication strategy, interfacial stability mechanism and potential application. *Critical Reviews in Food Science and Nutrition* 2024; **64(6)**, 1677-1700.

[47] YZ Shen, YS Ding, Q Gu and KC Chou. Identifying the hub proteins from complicated membrane protein network systems. *Medicinal Chemistry* 2010; **6(3)**, 165-173.

[48] K Vandereyken, J Van Leene, B De Coninck and BPA Cammue. Hub protein controversy: Taking a closer look at plant stress response hubs. *Frontiers in Plant Science* 2018; **9**, 694.

[49] Y Yao, Q Zhang, Z Li and H Zhang. MDM2: Current research status and prospects of tumor treatment. *Cancer Cell International* 2024; **24(1)**, 170.

[50] T Rajasegaran, CW How, A Saud, A Ali and JCW Lim. Targeting inflammation in non-small cell lung cancer through drug repurposing. *Pharmaceuticals* 2023; **16(3)**, 451.

[51] N Bhattacharyya, S Gupta, S Sharma, A Soni, SA Bagabir, M Bhattacharyya, A Mukherjee, AH Almalki, MF Alkhanani, S Haque, AK Ray and MZ Malik. CDK1 and HSP90AA1 appear as the novel regulatory genes in non-small cell lung cancer: a bioinformatics approach. *Journal of Personalized Medicine* 2022; **12(3)**, 393.

[52] S Chattopadhyay, SS Sarkar, S Saproo, S Yadav, D Antil, B Das and S Naidu. Apoptosis-targeted gene therapy for non-small cell lung cancer using chitosan-poly-lactic-co-glycolic acid-based nano-delivery system and CASP8 and miRs 29A-B1 and 34A. *Frontiers in Bioengineering and Biotechnology* 2023; **11**, 1188652.

[53] S Liu, J Liu, Y Wang, F Deng and Z Deng. Oxidative stress: Signaling pathways, biological functions, and disease. *MedComm* 2025; **6(7)**, e70268.

[54] EN Mendoza, MR Ciriolo and F Ciccarone. Hypoxia-induced reactive oxygen species: Their role in cancer resistance and emerging therapies to overcome it. *Antioxidants* 2025; **14(1)**, 94.

[55] K Tahayneh, M Idkedek and FA Akar. NSCLC: Current evidence on its pathogenesis, integrated treatment, and future perspectives. *Journal of Clinical Medicine* 2025; **14(3)**, 1025.

[56] LM Mustachio, A Chelariu-Raicu, L Szekvolgyi and J Roszik. Targeting KRAS in cancer: Promising therapeutic strategies. *Cancers* 2021; **13(6)**, 1204.

[57] R Lin and J Lin. Blocking of CDC25B suppresses sarcoma progression via arresting cell cycle. *Translational Cancer Research* 2025; **14(6)**, 3438-3451.

[58] I Pellarin, A Dall'Acqua, A Favero, I Segatto, V Rossi, N Crestan, J Karimbayli, B Belletti and G Baldassarre. Cyclin-dependent protein kinases and cell cycle regulation in biology and disease. *Signal Transduction and Targeted Therapy* 2025; **10(1)**, 11.

[59] X Yuan and D Xu. Telomerase reverse transcriptase (TERT) in action: Cross-talking with

epigenetics. *International Journal of Molecular Sciences* 2019; **20(13)**, 3338.

[60] F Chen, M Xiao, S Hu and M Wang. Keap1-Nrf2 pathway: A key mechanism in the occurrence and development of cancer. *Frontiers in Oncology* 2024; **14**, 1381467.

[61] TKH Lim, F Skoulidis, KM Kerr, MJ Ahn, JR Kapp, FA Soares and Y Yatabe. KRAS G12C in advanced NSCLC: Prevalence, co-mutations, and testing. *Lung Cancer* 2023; **184**, 107293.

[62] I Müller, E Strozyk, S Schindler, S Beissert, HZ Oo, T Sauter, P Lucarelli, S Raeth, A Hausser, NA Nakouzi, L Fazli, ME Gleave, H Liu, HU Simon, H Walczak, DR Green, J Bartek, M Daugaard and D Kulms. TRAIL-R2 promoting melanoma progression by inducing membrane ruffling and cell migration is regulated by interaction with TRAF2. *Cell Death & Disease* 2024; **15(1)**, 82.

[63] A Zafar, MJ Khan and A Naeem. MDM2 - An indispensable player in tumorigenesis. *Molecular Biology Reports* 2023; **50(8)**, 6871-6883.

[64] KT Skinner, AM Palkar and AL Hong. Genetics of ABCB1 in cancer. *Cancers* 2023; **15(17)**, 4236.

[65] K Jin, C Qian, J Lin and B Liu. Cyclooxygenase-2-prostaglandin E2 pathway: A key player in tumor-associated immune cells. *Frontiers in Oncology* 2023; **13**, 1099811.